Do Not Use Principal Components Analysis (PCA) for Prediction Problems, LOL is Typically Better

Joshua T. Vogelstein, Minh Tang, Da Zheng, Randal Burns, Mauro Maggioni

Abstract

It is increasingly common to acquire scientific data with hundreds, millions, or billions of features. The goal of these massive datasets is often to discover directions (or dimensions) that separate the data into two classes (for example, healthy and diseased). Unfortunately, when the dimensionality of the feature set is larger than the sample size, there are an infinite number of equally good options. Moreover, directly finding a small set of dimensions that maximize classification accuracy is computationally intractable. Instead, the nearly ubiquitous approach is to utilize Principal Components Analysis (PCA) to find a low-dimensional representation of the features that maximize variance. However, in general there is no reason to suspect that the dimensions that maximize classification accuracy will be close to those that maximize variance. Indeed, we show that, under reasonable assumptions, those two sets of directions will be approximately independent. To mitigate this issue, we developed a closed-form method called "Linear Optimal Low-rank" embedding (LOL), which extends PCA by by jointly utilizing both the dimensions that maximize classification accuracy (ignoring the variance) and the dimensions that maximize variance (ignoring the classification task). We show via a combination of theoretical results and simulations that LOL finds a better low-dimensional representation of the data for subsequent classification under relatively general settings, meaning that no matter what the dimensionality of the original data, or the dimensionality of embedded data, or sample size, LOL finds a better representation of the data for subsequent classification, while adding negligible additional computational cost. Additional numerical experiments demonstrate that the same intuition may fruitfully be applied to hypothesis testing and regression. We demonstrate the performance of LOL on three different applications: (i) sparse genetics, (ii) dense images, and (iii) connectomics application with over 500 million features comprising $>$400 gigabytes. In each case, LOL outperforms the other methods, while only requiring a few minutes on a single machine to run even on the huge dataset. Our open source implementation of LOL is easy to use, and computationally efficient, making it poised to tackle supervised dimensionality reduction challenges across disciplines.

Supervised learning—the art and science of estimating statistical relationships using labeled training data—is a crucial tool in scientific discovery. Supervised learning has been enabled a wide variety of basic and applied findings, ranging from discovering biomarkers in omics data [**?**] to object recognition from images [**?**]. A special case is classification; a classifier predicts the "class" of a novel observation via partitioning the space of observations (for example, predicting male or female from MRI scans). One of the most foundational and important approaches to classification is called "Fisher's Linear Discriminant Analysis" (LDA) [1]. LDA has a number of highly desirable properties for a reference classifier. First, it is built based on very simple geometric reasoning: when the data are Gaussian, all the information is in the means and variances, so the optimal classifier uses both the means and the variances. Second, due to its simplicity, LDA can be applied to multiclass problems, and can easily be extended to other problems. Third, theorems guarantee that when sample size is large, and dimensionality is small, LDA converges to the optimal classifier under the Gaussian assumption. And finally, again, because it is so simple, algorithms for implementing it are highly efficient.

Modern scientific datasets, however, present challenges for classification that were not addressed in Fisher's era. Specifically, the dimensionality of datasets is quickly ballooning. Currently, across many scientific disciplines, the raw data might consist of hundreds of millions of features or dimensions; for example, an entire genome or connectome. While the dimensionality of these data have increased precipitously, the sample sizes have not witnessed a concomitant increase. This "large p, small n" problem is disastrous for many classical statistical approaches because they were designed with "small p, large n" in mind. LDA in particular estimates a hyperplane in $p-1$ dimensions when the data are p dimensional. But there are an infinite number of $p-1$ dimensional hyperplanes that fit the data exactly when $p > n$. To visualize this, imagine fitting a line to a single point, or a plane to two points. In each case, one can choose any rotation, and still

fit the data perfectly. Therefore, without further constraints, algorithms will "over-fit", effectively randomly choose one of the many equally good fits, typically yielding a line or plane that is far from the optimal one. Supervised manifold learning is field devoted to combating this this over-fitting issue by searching for a small number of dimensions that maximize predictive accuracy. Two complementary strategies have been pursued.

Perhaps the most prominent strategy is to use principal components analysis (PCA) [**?**] to "pre-process" the data, that is, to reduce the dimensionality of the data prior to a subsequent classification using the much lower dimensional data. While hugely successful, PCA is a wholly *unsupervised* dimensionality reduction technique, meaning that PCA does not utilize the class labels while learning the low dimensional representation. This results in dimensions that have no statistical guarantee of being close to the best ones, and in fact, as we show below, with high probability will be completely wrong. Other unsupervised nonlinear dimensionality reduction techniques, called manifold learning, are ill-equipped to address this problem because they typically only learn a low-dimensional representation for a set of points; thus, they are unable to be applied to new test data. Moreover, they often require costly numerical methods that do not scale, and lack theoretical justification in this setting.

A different strategy that focuses on utilizing the class label information is called "sparsity". Sparse methods find a small subset of the original features to use for subsequent inference [**?**]. There are many such approaches (often called "feature selection" or "feature screening"); the advantage of these approaches is that the result is sometimes more easily interpretable. The disadvantage, however, is that exactly solving the problem is computationally intractable, requiring time that increases exponentially in the number of features. Various approximations enable efficient algorithms that have provable guarantees under certain limiting assumptions. LASSO is a particularly popular algorithm that has these properties. Unfortunately, LASSO cannot run on millions of dimensions, it has a hyper-parameter that requires careful tuning, and often produces spurious answers even when the unrealistically strict assumptions are met [**?**]. A more recent approach is called "regularized optimal affine discriminant" (ROAD). ROAD finds the optimal sparse dimensionality reduction under certain Gaussian assumptions. ROAD, however, can only be applied in two-class settings, and requires solving a computationally costly numerical optimization problem, and thus does not scale to large dimensionality.

There is therefore a gap: the field lacks the high-dimensional analog of Fisher's LDA, that is, a method based on simple geometric intuition, that can be applied to multiclass and more general problems, with theorems that guarantee good performance for arbitrarily large dimensionality, and an efficient implementation that scales to hundreds of millions of features. To address these concerns, we developed "Linear Optimal Low-rank" embedding (LOL). The key intuition behind LOL is that we can jointly utilize both directions that are informative with regard to the classification task (the means) and the directions that maximize the variance (the covariance), much like LDA. But by virtue of utilizing random matrix theory, we are able to prove that LOL finds a better low dimensional representation than PCA and other linear methods under the Gaussian assumption. This is true regardless of the dimensionality of the features, the number of samples, and the number of dimensions in which we project. Numerical experiments quantitatively demonstrate the improvement of LOL over reference methods on a wide range of simulated experiments that both satisfy our theoretical assumptions, and go beyond them. In fact, one can extend LOL outside of classification problems to regression and hypothesis testing and obtain qualitatively similar results. Computationally, LOL is always numerically stable, and requires no more computational space, and smaller computational time, than other linear methods. Moreover, we provide a highly scalable implementation that efficiently runs on datasets with hundreds of millions of features comprising hundreds of gigaabytes. We then tested LOL against a set of standard methods on several benchmark datasets: there was not a single method that outperformed LOL in any dimension. We provide open source implementations of LOL in both MATLAB and R to support further applications and extensions.

This work therefore makes four complementary challenges to the machine learning literature. First, we provide geometric intuition for how supervised manifold learning methods can work, suggestive of potential algorithms. Second, we provide one example algorithm that satisfies the desiderata, specifically that is simple enough to admit theoretical investigations and efficient implementations. Third, we provide a theoretical framework for evaluating supervised manifold learning for classification that does not depend on

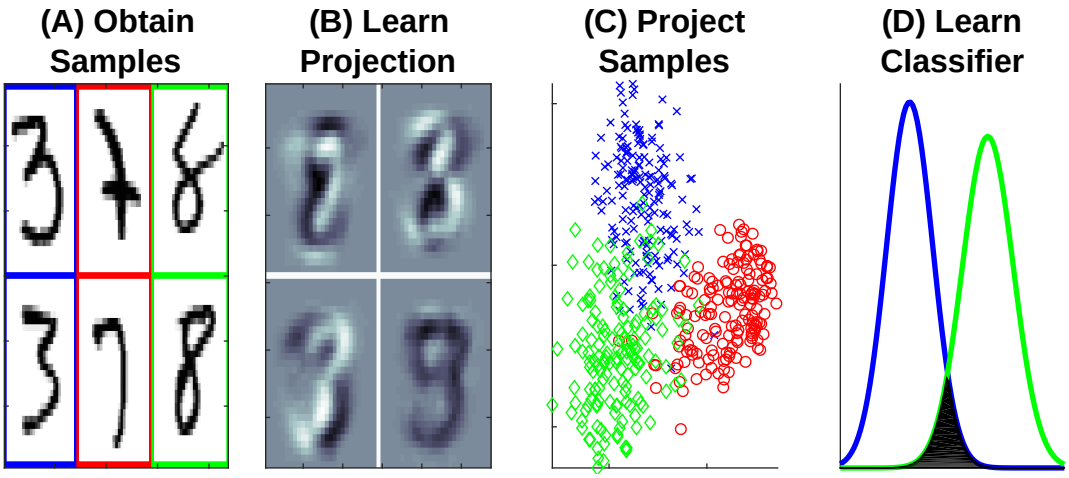

Figure 1: Schematic illustrating Linear Optimal Low-rank Embedding as a supervised manifold learning technique. **(A)** 300 training samples of the numbers 3, 7, and 8 from the MNIST dataset (100 samples per digit); each sample is a 28 $\times$ 28 = 784 dimensional image (boundary colors are for visualization purposes). **(B)** The first four projection matrices learned by LOL. Each is a linear combination of the sample images. **(C)** Projecting 500 new (test) samples into the top two learned dimensions; digits color coded as in (A). LOL embedded data form three distinct clusters. **(D)** Use the low-dimensional data to learn a classifier. The estimated distributions for 3 and 8 of test samples after projecting data into two dimensions and using LDA to classify demonstrate that 3 and 8 are easily separable by linear methods after LOL projections (color of line indicates the digit). The filled area is the estimated error rate; the goal of any classification algorithm is to minimize that area. LOL is performing well on this high-dimensional real data example.

the subsequent classifier. And fourth, we provide a scalable implementation that can run on half-terabyte datasets on single machines in a few minutes. The arguments and methodology developed herein provide a comprehensive framework for developing big supervised manifold learning algorithms to tackle other data science challenges.

Supervised Manifold Learning

A general strategy for supervised manifold learning is schematiized in Figure 1. Step **(A)**, obtain or select n training samples of high-dimensional data. For concreteness, we utilize one of the most popular benchmark datasets, the MNIST dataset [2]. This dataset consists of $n = 60{,}000$ examples of images of the digits 0 through 9. Each such image is represented by a 28×28 matrix, which means that the observed dimensionality of the data is $p = 28^2 = 784$. Because we are motivated by the $n \ll p$ scenario, we subsample the data to select $n = 300$ examples of the numbers 3, 7, and 8 (100 of each). Step **(B)**, learn a "projection" that maps the high-dimensional data to a low dimension representation. One can either ignore the class label data, that is, ignore which images correspond to which digits (as PCA and most manifold learning techniques do), or try to use them (as sparse methods do). LOL uses the class labels to learn projections that are linear combinations of the original data samples (panel B shows the first four projections that LOL learns, each of which looks like a combination of the original images). Step **(C)**, use the learned projections to map the high-dimensional data into the lower dimensional space. This step requires having learned a projection that can be applied to new (test) data samples for which we do not know the true class labels. Nonlinear manifold learning methods typically are unable to be applied in this way (see for example, **?**]). LOL, however, can project new samples in such a way as to separate the data into classes (in panel C, two-dimensional points represent the original images, color coded by their digit label, are well separated). Finally, step **(D)**, using the low-dimensional representation of the data, learn a classifier. A good classifier correctly identifies as many points as possible with the correct label. Panel D shows that when using LDA on the low-dimensional data from LOL, the data points are mostly linearly separable. Specifically, the two curves correspond to the distribution of 3's (in blue) and 8's (in green) after applying LDA to the data projected using LOL, and the area of overlap (in black) corresponds to the fraction of errors, so smaller is better.

Linear Gaussian Intuition

To build intuition about when LOL performs well, and when it does not, we consider the simplest high-dimensional classification setting. We observe n samples $(\boldsymbol{x}_i, y_i)$, where $\boldsymbol{x}_i$ are p dimensional feature vectors, and y_i is the binary class label, that is y_i is either 0 or 1. We assume that both classes are distributed according to a multivariate Gaussian distribution, and the two classes have the same covariance matrix $\boldsymbol{\Sigma}$ and data from either class is equally likely, so that the only difference between the classes is their means, $\boldsymbol{\mu}^1$ and $\boldsymbol{\mu}^2$. The optimal low-dimensional projection is analytically available in this scenario—commonly referred to as Fisher's Linear Discriminant Analysis (LDA)—it is the dot product of the difference of means and the inverse covariance matrix, $(\boldsymbol{\mu}^1 - \boldsymbol{\mu}^2)^\mathsf{T}\boldsymbol{\Sigma}^{-1}$ [3] (see Methods for derivation). When the distribution of the data are unavailable, as in all real data problems, machine learning methods estimate the parameters instead. Unfortunately, when $n < p$, the estimated covariance matrix will not be invertible, so analysts must use something else. For example, PCA utilizes the pooled sample mean, $\hat{\boldsymbol{\mu}} = \frac{1}{n}\sum_{i=1}^{n} \boldsymbol{x}_i$ and the pooled sample covariance matrix, $\hat{\boldsymbol{\Sigma}}$ with entries $\hat{\boldsymbol{\Sigma}}_{kl} = \frac{1}{n}\sum_{i=1}^{n}(x_{ik} - \mu_k)(x_{il} - \mu_l)$. The PCA projection is the top d eigenvectors of the pooled sample covariance matrix, thus completely ignoring the class labels.

The key insight of our work is that we can combine the class means and the covariance matrix in a simple fashion, rather than just the covariance matrix, to find a low dimensional projection. This is motivated by Fisher's LDA, which utilizes both means and variance, and should therefore improve performance over PCA which only utilizes the variances. More specifically, for a two-class problem, LOL first computes the sample mean of each class, $\hat{\boldsymbol{\mu}}^j = \frac{1}{n_j}\sum_{i:y_i=j} \boldsymbol{x}_i$, where n_j is the number of samples in class j. Second, LOL estimates the difference between means, $\hat{\boldsymbol{\delta}} = \hat{\boldsymbol{\mu}}^1 - \hat{\boldsymbol{\mu}}^2$. Third, LOL computes the class-conditional covariance matrix, $\widetilde{\boldsymbol{\Sigma}}$ with entries $\widetilde{\boldsymbol{\Sigma}}_{kl} = \sum_{j=1}^{J}\frac{1}{n}\sum_{i:y_i=j}(x_{ik} - \mu_k^j)bx_{il} - \mu_l^j)$. In other words, LOL centers each data point with respect to its own classes mean, rather than the overall pooled mean, and then computes the covariances. Fourth, LOL computes the eigenvectors of this class-conditionally centered covariance. And finally, LOL simply concatenates the difference of the means with the top $d-1$ eigenvectors of $\widetilde{\boldsymbol{\Sigma}}$. Note that the sample class-conditional covariance matrix estimates the population covariance, $\boldsymbol{\Sigma}$, whereas the sample pooled covariance matrix is distorted by the difference of the class means. All together, LOL estimates both the difference of the means and the covariance matrix, just like Fisher's LDA.

Figure 2 shows three different examples of data sampled from the Gaussian model to geometrically illustrate this intuition (see Methods for details). In each, the top row shows, for $n = 100$ training samples, the first two dimensions of a $p = 1000$ dimensional space, so $n \ll p$. The next four rows each show the distribution of test data after using LDA on the low-dimensional representation (solid line for class 0 and dashed line for class 1, and the vertical line is the estimated boundary between the two classes).

Figure 2A shows an example we call "stacked cigars". In this example all dimensions are uncorrelated with one another. Moreover, the difference between the means and direction of maximum variance are both large along the same dimension. This is an idealized setting for PCA, because PCA finds the direction of maximal variance, which happens to correspond to the direction of maximal separation of the classes. We also compare this to a method we refer to as PCA'. which uses the top d eigenvectors of the sample class-conditional covariance matrix, $\widetilde{\boldsymbol{\Sigma}}$. As it turns out, composing this projection with LDA is equivalent to a method called "Reduced Rank LDA" [**?**] (see Appendix **??** for proof). PCA' performs well here too, for the same reason that PCA does. Because all dimensions are uncorrelated, and one dimension contains most of the information discriminating between the two classes, this is a good scenario for sparse methods. Indeed, ROAD, a sparse classifier designed for precisely this scenario, does an excellent job finding the most useful dimensions [**?**]. LOL, using both the difference of means and the directions of maximal variance also does well. To calibrate all of these methods, we also show the performance of the optimal classifier.

Figure 2B shows an example which is worse for PCA. In particular, the variance is getting larger for subsequent dimensions, $\sigma_1 < \sigma_2 < \cdots < \sigma_p$, while the magnitudes of the difference between the means are decreasing with dimension, $\delta_1 > \delta_2 < \cdots > \delta_p$. Because PCA operates on the pooled sample covariance matrix, the dimensions with the maximum difference are included in the estimate, and therefore, PCA finds some of them, while also finding some of the dimensions of maximum variance, therefore performing fairly well. PCA', however, by virtue of subtracting out the difference of the means, is now completely at chance performance. ROAD is not hampered by this problem, it is also able to find the directions of maximal discrim-

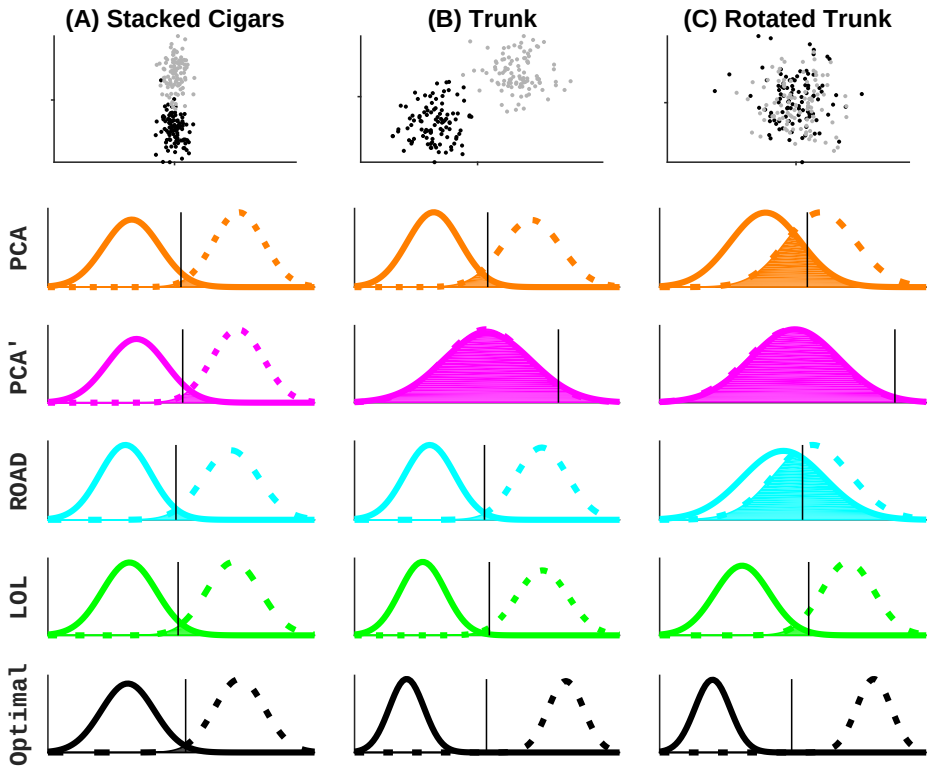

Figure 2: LOL achieves near optimal performance for a wide variety of Gaussian distributions. Each point is sampled from a multivariate Gaussian; the three columns correspond to different simulation parameters (see Methods for details). In each of 3 simulations, we sample $n = 100$ points in $p = 1000$ dimensions, so $n \ll p$. And for each approach, we embed into the top 20 dimensions. Note that we use the sample estimates, rather than the true population values of the parameters. The five columns show (in decreasing order): **Row 1**: A scatter plot of the first two dimensions of the sampled points, with class 0 and 1 as black and gray dots, respectively. **Row 2** - **Row 5**: the posteriors after projecting using different manifold learning techniques, including **Row 2** PCA. **Row 3** PCA', a method that projects onto the top d eigenvectors of sample class-conditional covariance [**?**], **Row 4** ROAD, a sparse method designed specifically for this model [4]. **Row 5** LOL, our proposed method. **Row6** the Bayes optimal classifier. **(A)** The mean difference vector is aligned with the direction of maximal variance, maxing it ideal for both PCA or RR-LDA to discover the discriminant dimension and a sparse solution. In this setting, the results are similar for all methods, and essentially optimal. **(B)** The mean difference vector is orthogonal to the direction of maximal variance, making PCA perform worse, RR-LDA is at chance, but sparse methods and LOL can still recover the correct dimensions, achieving nearly optimal performance. **(C)** Same as B, but the data are rotated, in this case, only LOL performs well. Note that LOL is closest to Bayes optimal in all three settings.

ination, rather than those of maximal variance. Again, LOL, by using both the means and the covariance, does extremely well.

Figure 2C is exactly the same as B, except the data have been randomly rotated in all 1000 dimensions. This means that none of the original coordinates have much information, rather, linear combinations of them do. This is evidenced by observing the scatter plot, which shows that the first two dimensions fail to disambiguate the two classes. PCA, being rotationally invariant, performs approximately as well in this scenario as in B. PCA' is not helped by this random rotation, so still performs at chance levels. Because there is no small number of features that separate the data well, ROAD fails. LOL performs nearly as well here as it does in the other examples.

Collectively, these three examples demonstrate when, based purely on geometric intuition, that LOL performs as expected in a variety of Gaussian settings.

Statistical Theory

The above numerical experiments provide the intuition to guide our theoretical developments.

Theorem 1. LOL *is always better than or equal to* PCA*' under the Gaussian model, and better than or equal to* PCA *with relatively weak conditions, as well as other linear projections. This is true for all possible observed dimensionality of the data, and number of dimensions into which we embed, for sufficiently large sample sizes. Moreover, under relatively weak assumptions, these conditions hold almost surely as the number of dimensions increases.*

A formal statement of the theorem and proof are provided in Appendix **??**. The condition for LOL to be better than PCA is essentially that the d^{th} eigenvector of the pooled sample covariance matrix has less information about classification than the difference of the means vector. The implication of the above theorem is that it is better to incorporate the mean difference vector into the projection matrix than not. The *degree* of improvement is a function of the embedding dimension d, the dimensionality of the feature set p, and the parameters (see Methods for details and proof), but the *existence* of an improvement, or at least no worse performance, is independent of those factors. It is worth specifying exactly what "better" means in this context. In this context, it is desirable to have a notion of better that is agnostic to the subsequent classifier, that is, a metric that quantifies how good an embedding in, no matter which classifier we will use. We utilized Chernoff Information to calculate the distance between the distributions after embedding. Chernoff information is fundamentally related to the expected classification error; specifically, it is the exponential convergence rate for the Bayes error.

Numerical Experiments Extending Our Theoretical Results

Here we numerically investigate the performance of LOL versus PCA and other methods empirically using simulations, both under the model assumptions for which our theorems hold, as well as more general assumptions for which we currently lack theory. For each of four different scenarios, we sample $n = 100$ training samples each with $p = 100$ features; therefore, FIsher's LDA cannot solve the problem because there are infinitely many ways to overfit. For each setting we evaluate the misclassification rate on held out data for all number of dimensions to embed into. The comparison algorithms are PCA, PCA', LASSO, and ROAD.

Theoretical model We begin by investigating two scenarios that satisfy the LDA model assumptions required by our proofs. FirstConsider the rotated trunk example from Figure 2C as well as a "Toeplitz" example, as depicted in Figures 3A and B, respectively. In both cases, we compare LOL to FLDOPCA and ROAD. In both scenarios, for all dimensions, LOL achieves a lower error rate than either of its competitors.

Multiple Classes LOL can trivially be extended to > 2 class situations. Naïvely it may seem like we would need to keep all pairwise differences between means. However, given k classes, the set of all k^2 differences is only rank $k - 1$. In other words, we can equivalently compute the distance of each mean to a single mean (in practice, for minimizing variance reasons, we use the class which has the maximum number of samples (breaking ties randomly). Figure 3C shows a 3-class generalization of the rotated Trunk example from Figure 3A. While LOL uses the additional class naturally, many previously proposed high-dimensional classifiers, such as ROAD, natively only work for 2-classes. Thus, we only compare LOL to FLDOPCA here. As before, LOL significantly outperforms FLDOPCA for all embedding dimensions.

Generalizations of LOL

The above simulations were all under the LDA model, for which we have theoretical guarantees that LOL should outperform FLDOPCA. In this section, we explore simulation settings that extend beyond the geometric constraints we required for our proofs, to develop an even deeper understanding of LOL.

Fat Tails Figure 3D shows a sparse example with "fat tails" to mirror real data settings better. More specifically, each class is the sum of multiple Gaussians, with the same mean, but different covariances (see Methods for details). The qualitative results are consistent with those of A and B, even though the setting is

no longer exactly the setting under which we have theoretical confirmation. More specifically, LOL outperforms FLDoPCA and ROAD for all dimensions.

QDA Sometimes, it makes more sense to model each class as having a unique covariance matrix, rather than a shared covariance matrix. Assuming everything is Gaussian, the optimal classifier in this scenario is called Quadratic Discriminant Analysis (QDA) [5]. Intuitively then, we can modify LOL to compute the eigenvectors separately for each class, and concatenate them (sorting them according to their singular values). Moreover, rather than classifying the projected data with LDA, we can then classify the projected data with QDA. Indeed, simulating data according to such a model (Figure 3E), LOL performs slightly better than chance, regardless of the number of dimensions we use to project, whereas QOQ (for Quadratic Optimal QDA) performs significantly better regardless of how many dimensions it keeps. This demonstrates a straightforward generalization of LOL, available to us because of the simplicity and intuitiveness of LOL.

Outliers Outliers persist in many real data sets. Finding outliers, especially in high-dimensional data, is both tedious and difficult. Therefore, it is often advantageous to have estimators that are robust to certain kinds of outliers [6–8]. PCA and eigenvector computation are particularly sensitive to outliers [9]. Because LOL is so simple and modular, we can replace typical eigenvector computation with a robust variant thereof, such as the geometric median subspace embedding [10]. Figure 3F shows an example where we generated $n/2$ training samples according to the simple LDA model, but then added another $n/2$ training samples from a noise model. LRL (Linear Robust Low-Rank), performs better than LOL regardless of the number of dimensions we keep. This simulation setting further demonstrates the flexibility of the LOL framework to be extensible to other, more complicated scenarios.

XOR XOR is perhaps the simplest nonlinear problem, the problem that led to the demise of the perceptron, prior to its resurgence after the development of multi-layer perceptrons [11]. Thus, in our opinion, it is warranted to check whether any new classification method can perform well in this scenario. The classical (two-dimensional) XOR problem is quite simple: the output of a classifier is zero if both inputs are the same (00 or 11), and the output is one if the inputs differ (01 or 10). Figure 3G shows a high dimensional and stochastic variant of XOR (see Methods for details). This simulation was designed such that standard classifiers, such as support vector machines and random forests, achieve chance levels (not shown). LOL, performs moderately better than chance, and QOQ performs significantly better than chance, regardless of the chosen dimensionality. This demonstrates that our classifiers developed herein, though quite simple and intuition, can perform well even in settings where the data are badly modeled by our underlying assumptions. This mirrors previous findings where the so-called "idiots's Bayes" classifier outperforms more sophisticated classifiers [3]. In fact, we think of our work as finding intermediate points between idiot's Bayes (or naïve Bayes) and FLD, by enabling degrees of regularization by changing the dimensionality used.

Computational Efficiency

In many applications, the main quantifiable consideration in whether to use a particular method, other than accuracy, is computational efficiency. Because implementing LOL requires only highly optimized linear algebraic routines—including computing moments and singular value decomposition—rather than the costly iterative programming techniques currently required for sparse or dictionary learning type problems. Moreover, because LOL only requires computing means and covariances, we can leverage recent advances in parallel matrix operations [12] on fast solid-state drives (SSDs). We implement LOL with the R interface of FlashX [12–14]. Given the FlashX programming framework, we can run LOL on essentially arbitrarily large data. For these examples, we simulated data satisfying the LDA model; specifically, we used a spherically symmetric covariance matrix, with means just $\pm$ the one vector (see Methods for simulation details).

Figure 4A demonstrates both the in memory and semi-external memory [15] computing models of our implementation. For the in memory implementation (light green line), we see that the run time increases linearly with the number of dimensions, requiring about 11 minutes to run LOL on a $p = 32{,}000{,}000$ dimensional problem with $n = 2000$ samples. This linear increase is the optimal scale up according to Ahmdel's Law [16]. This example already requires 477 gigabyte (GB) to store the data, but $<$1 GB to perform the computations. For larger data, we developed a semi-external memory implementation, which stores the

data matrix on solid state drives, and the low-rank estimates in RAM [17]. This strategy allows us to run LOL as long as the data can fit on disk, and the low-rank approximation can fit in RAM. The semi-external memory implementation (dark green line) achieves the same performance as the in memory implementation whenever the data are small enough for in memory, and continues scaling optimally (linearly) as the dimensionality further increases to $p = 128,000,000$ dimensions, a multi-terabyte scenario.

Another option for making LOL scale up better is to utilize randomized algorithms. In particular, random projections—for which the data are multiplied by a lower-dimensional random matrix—have been shown to provide excellent approximation eigenvectors [18]. Moreover, very sparse random projections, in which the elements of the matrix are mostly zero, with ± 1 randomly distributed, have been shown to be effective, and have significant computational benefits [19]. We therefore further modified FlashX to incorporate random projections and very sparse random projections, and let LAL denote Linear Approximate Low-rank. Figure 4A shows an order of magnitude improvement in both the in-memory and semi-external memory implementations of LAL.

Figure 4B shows the error for LOL and FLDOPCA in this scenario, simply to demonstrate that even in this extremely high dimensional setting, LOL still outperforms FLDOPCA. As expected, LAL performs as well as Lol for the low dimensional settings.

Computational Theory

We reify the above computational experiments with theoretical statements. Computing the mean for each class requires $\mathcal{O}(n_j p)$ floating point operations (flops), where n_j is the number of samples per class. Subtracting the means requires $\mathcal{O}((J-1)p)$ flops, where J is the total number of classes. Computing the first d singular triples (left and right singular vectors, and singular value) requires $\mathcal{O}(npd)$ flops. The sparse random projection however only requires $\mathcal{O}(npd/c)$, where $c1$ is the sparsity of the sparse random projection matrix. Since, $d \ll n, p$, this can substantially reduce computational complexity. Regardless, LOL computation is clearly bottlenecked by the PCA computation or random projection for single threaded operations.

Our parallel in memory implementation scales-up optimally (linearly) with the number of threads, requiring $\mathcal{O}(npd/T)$ flops for LOL, and $\mathcal{O}(npd/cT)$ flops for LAL, where T is the number of threads. Our parallel semi-external memory implementation scales-out optimally (linearly) as well. This is in agreement with the linear fit of the lines in Figure 4A.

Benchmark Real Data Applications

Although LOL both statistically and computationally outperforms its natural competitors both in theory and in a variety of simulation settings, real data often tell a different story. We have therefore selected four commonly used high-dimensional datasets to compare LOL to several state-of-the-art algorithms (see Methods for details). For each dataset, we compare LOL to (i) support vector machines (SVM), (ii) ROAD, (iii) lasso, (iv) and random forest (RF). Because in practice all these approaches have "hyperparameters" to tune, we consider several possible values for SVM, lasso, and LOL (but not RF, as its runtime was too high). Figure 5 shows the results for all four datasets. For each, we use MATLAB implementations, partially because ROAD provides MATLAB code, and also because of MATLAB's ubiquity in certain communities. Because we also have R and FlashX implementations of LOL, comparisons using other languages would be straightforward.

Qualitatively, the results are similar across datasets: LOL achieves high accuracy and computational efficiency as compared to the other methodologies. Considering Figure 5A and B, two popular sparse settings, we find that LOL can find very low dimensional projections with very good accuracy. For the prostate data, with a sufficiently non-sparse solution for ROAD, it slightly outperforms LOL, but at substantial computational cost; in particular, ROAD takes about 100 times longer to run on this dataset. Figure 5C and D are 10-class problems, so ROAD is no longer possible. Here, SVM can again slightly outperform LOL, but again, requiring 100 fold additional computational time. In all cases, the beloved random forest classifier performs subpar. In all four scenarios, there is never an algorithm that achieves smaller error in less time, as indicated by the dark gray box being empty in the lower panels of Figure 5A-D.

Extensions to Other Supervised Learning Problems

The utility of incorporating the mean difference vector into supervised machine learning for big and wide data extends beyond merely classification. In particular, hypothesis testing can be considered as a special case of classification, with a particular loss function. Therefore we apply the same idea to a hypothesis testing scenario. The multivariate generalization of the t-test, called Hotelling's Test, suffers from the same problem as does the classification problem; namely, it requires inverting an estimate of the covariance matrix whose estimate would be low-rank and therefore singular, in the high-dimensional setting. To mitigate this issue in the hypothesis testing scenario, prior art applied similar tricks as they have done in the classification setting. One particularly nice and related example is that of Lopes et al. [20], who addresses this dilemma by using random projections to obtain a low-dimensional representation, following by applying Hotelling's Test in the lower dimensional subspace. Figure 6A and B shows the power of their test alongside the power of the same approach, but using the LOL projection rather than random projections. The two different simulations include the simulated settings considered in their manuscript (see Methods for details). The results make it clear that the LOL test has higher power for essentially all scenarios. Moreover, it is not merely the replacing random projections with PCA (solid magenta line), nor simply incorporating the mean difference vector (dashed green line), but rather, it appears that LOL for testing uses both modifications to improve performance.

High-dimensional regression is another supervised learning method that can utilize the LOL idea. Linear regression, like classification and Hotelling's Test, requires inverting a matrix as well. By projecting the data only a lower dimensional subspace first, followed by linear regression on the low-dimensional data, we can mitigate the curse of high-dimensions. To choose the projection matrix, we partition the data into K partitions, based on the percentile of the target variable, we obtain a K class classification problem. Then, we can apply LOL to learn the embedding. Figure 6C shows an example of this approach, contrasted with LASSO and partial least squares, in a sparse simulation setting (see Methods for details). LOL is able to find a better low-dimensional projection than LASSO, and performs significantly better than partial least squares, for essentially all choices of number of dimensions to embed into.

Discussion

We have introduced a very simple, yet new, methodology to improve performance on supervised learning problems with big and wide data. In particular, we have proposed a supervised manifold learning procedure that utilizes both the difference of the means, and the covariance matrices, and proved that it performs better than first applying PCA to the data under reasonable assumptions. This is in stark contrast to most previous approaches, which only utilize the covariance matrices (or kernel variants thereof), or try to solve a difficult optimization theoretic problem. In addition to demonstrating the statistical accuracy and computational efficiency of LOL on simulated and real classification problems, we also demonstrate how the same idea can also be used for other kinds of supervised learning problems, including regression and hypothesis testing. Theoretical guarantees suggest that this line of research is promising and can be extended to other more general settings and tasks.

Related Work One of the first publications to compose FLD with an unsupervised learning method was the celebrated Fisherfaces paper [21]. The authors showed via a sequence of numerical experiments the utility of embedding with PCA prior to classifying with FLD. We extend this work by adding a supervised component to the initial embedding. Moreover, we provide the geometric intuition for why and when this is advantageous, as well as show numerous examples demonstrating its superiority. We also prove that Fisherfaces can be implemented very efficiently (see Methods), while shedding light on why it is performing relatively well in general.

Next Steps The LOL idea, appending the mean difference vector to convert unsupervised manifold learning to supervised manifold learning, has many potential applications. We have presented the first few. Incorporating additional nonlinearities via kernel methods [22], ensemble methods such as random forests [23], and multiscale methods [24] are all of immediate interest. MATLAB, R, and FlashR code for the experiments performed in this manuscript is available from http://docs.neurodata.io/LOL/.

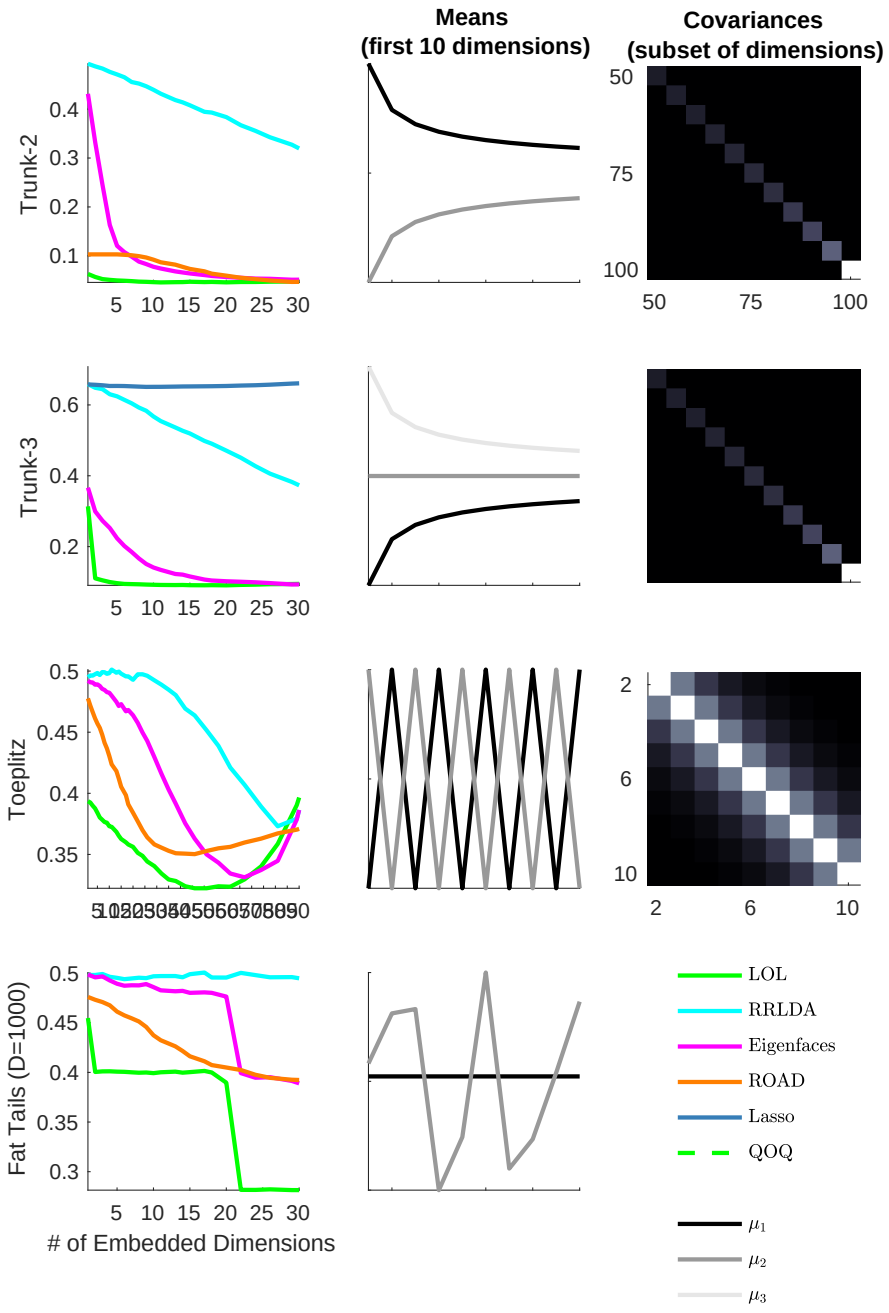

Figure 3: Seven simulations demonstrating LOL achieves superior finite sample performance over competitors both in settings for which we have asymptotic theoretical guarantees, and those for which we do not. For the first three, the top panels depict the means (top), the shared covariance matrix (middle). For the next three, the top panels depict a 2D scatter plot (left), mean and level set of one standard deviation of covariance matrix (right). For all seven simulations, the bottom panel shows misclassification rate as a function of the number of embedded dimensions, for several different classifiers. The simulations settings are as follows: **(A)** Rotated Trunk: same as Figure 2C. **(B)** Toeplitz: another setting where mean difference is not well correlated with any eigenvector, and no ambient coordinate is particularly useful on its own. **(C)** 3 Class variant of the rotated Trunk example to demonstrate that LOL naturally adapts, and excels in, multi-class problems. **(D)** Fat Tails: a common phenomenon in real data that is more general than our theory supports. **(E)** QDA: QOQ, a variant of LOL when each class has a unique covariance, outperforms LOL, as expected, when the true discriminant boundary is a quadratic, rather than linear, function. **(F)** Outliers: adding high-dimensional outliers degrades performance of standard eigensolvers, but those can easily be replaced in LOL for a robust variants (called LRL). **(G)** XOR: a high-dimensional stochastic generalization of XOR, demonstrating that QOQ works even in scenarios that are quite distinct from the original motivating problems. In all 7 cases, LOL, or the appropriate generalization thereof, outperforms unsupervised or sparse methods. Moreover, the optimal embedding dimension is never the true discriminant dimension, but rather, a smaller number jointly determined by parameter settings and sample size.

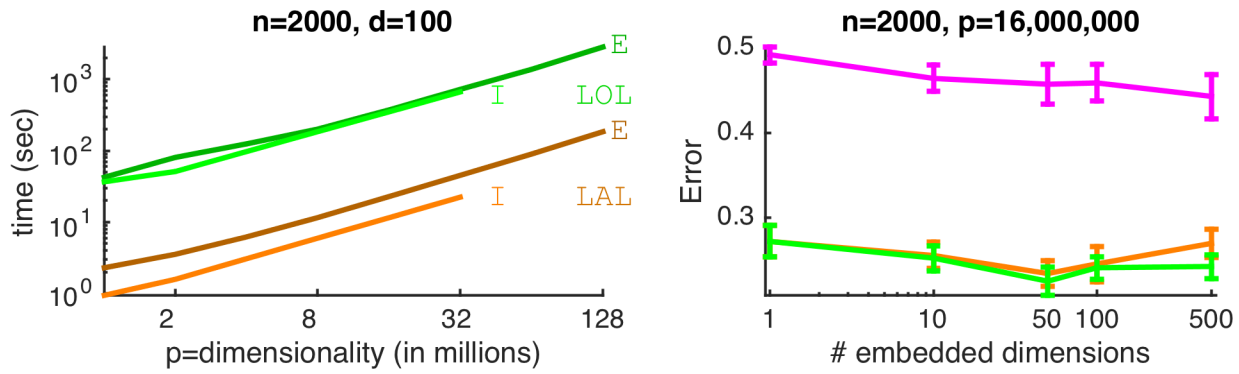

Figure 4: Computational efficiency of various low-dimensional projection methods. In all cases, $n = 2000$, and we used spherically symmetric simulation parameters (see Methods for details). We compare PCA with the projection step of LOL (light green for in memory, dark green for semi-external memory) and LFL (light orange for in-memory, dark orange for semi-external memory) for different observed dimensions (p). **(A)** LOL exhibits optimal (linear) scale up and scale out, requiring only 46 minutes to find the embedding on a 2TB dataset, and only 3 minutes using LAL(the sparse constant of sparse random projection $c = \frac{1}{\sqrt{p}}$). **(B)** Error for LAL is the same as LOL in this setting, and both are significantly better than FLDOPCA for all choices of embedding dimension.

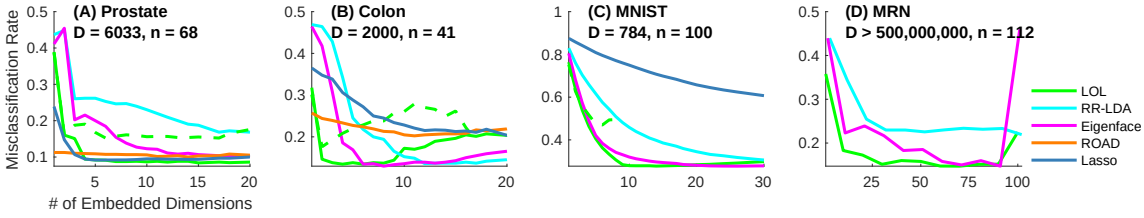

Figure 5: For four standard datasets, we benchmark LOL (green circles) versus standard classification methods, including support vector machines (blue up triangles), ROAD (cyan down triangles), LASSO (magenta pluses), and random forest (orange diamonds). Top panels show error rate as a function of $\log_2$ number of embedded dimensions (for LOL, ROAD, and LASSO) or cost (for SVM). Bottom panels show the minimum error rate achieved by each of the five algorithms versus time. The lower left dark gray (upper right light gray) rectangle is the area in which any algorithm is *better* (worse) than LOL in terms of both accuracy and efficiency. **(A)** Prostate: a standard sparse dataset. 1-dimensional LOL does very well, although keeping 2^5 ambient coordinates slightly improves performance, at a significant cost of compute time (two orders of magnitude), with minimal additional interpretability. **(B)** Colon: another standard sparse dataset. Here, 2-4 dimensions of LOL outperforms all other approaches considered regardless of how many dimensions they keep. **(C)** MNIST: 10 image categories, so ROAD is not possible. LOL does very well regardless of the number of dimensions kept. SVN marginally improves on LOL accuracy, at a significant cost in computation (two orders of magnitude). **(D)** CIFAR-10: a higher dimensional and newer 10 category image classification problem. Results are qualitatively similar to C. Note that, for all four of the problems, there is no algorithmperforming better and faster than LOL; rather, most algorithms typically perform worse and slower (though some are more accurate and much more computationally expensive).

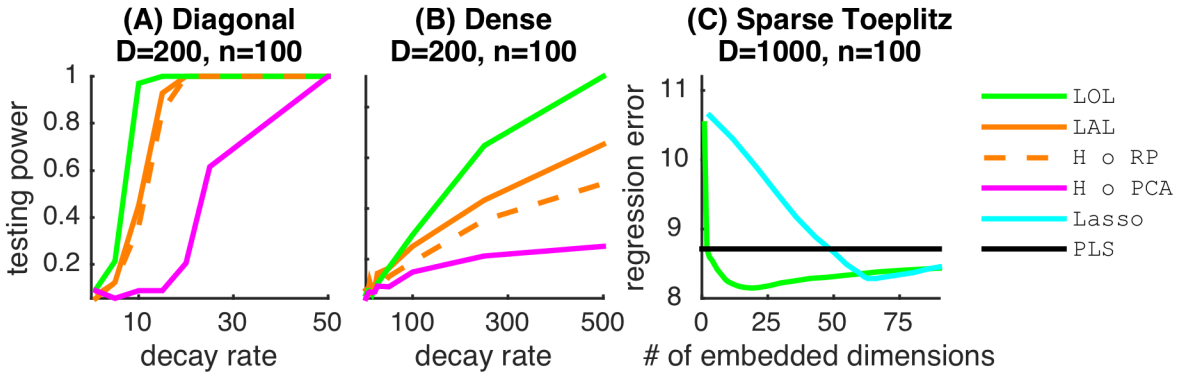

Figure 6: The intuition of including the mean difference vector is equally useful for other supervised manifold learning problems, including testing and regression. **(A)** and **(B)** show two different high-dimensional testing settings, as described in Methods. Power is plotted against the decay rate of the spectrum, which approximates the effective number of dimensions. LOL composed with Hotelling's test outperforms the random projections variants described in [20], as well as several other variants. **(C)** A sparse high-dimensional regression setting, as described in Methods, designed for sparse methods to perform well. Log_{10} mean squared error is plotted against the number of embedded dimensions. LOL composed with linear regression outperforms LASSO (cyan), the classic sparse regression method, as well as partial least squares (PLS; black). These three simulation settings therefore demonstrate the generality of this technique.

A Simulations

For most simulation settings, each class is Guassian: $f_{x|y} = \mathcal{N}(\boldsymbol{\mu}_y, \boldsymbol{\Sigma}_{\boldsymbol{y}})$, $f_y = \mathcal{B}(\pi)$. We typically assume that both classes are equally like, $\pi = 0.5$, and the covariance matrices are the same, $\boldsymbol{\Sigma}_0 = \boldsymbol{\Sigma}_1 = \boldsymbol{\Sigma}$. Under such assumptions, we merely specify $\boldsymbol{\theta} = \{\boldsymbol{\mu}_0, \boldsymbol{\mu}_1, \boldsymbol{\Sigma}\}$.

Stacked Cigars

- $\boldsymbol{\mu}_0 = \mathbf{0}$,
- $\boldsymbol{\mu}_1 = (a, b, a, \ldots, a)$,
- $\boldsymbol{\Sigma}$ is a diagonal matrix, with diagonal vector, $\boldsymbol{d} = (1, b, 1 \ldots, 1)$,

where $a = 0.15$ and $b = 4$.

Trunk

- $\boldsymbol{\mu}_0 = b/\sqrt{(1, 3, 5, \ldots, 2p)}$,
- $\boldsymbol{\mu}_1 = -\boldsymbol{\mu}_0$,
- $\boldsymbol{\Sigma}$ is a diagonal matrix, with diagonal vector, $\boldsymbol{d} = 100/\sqrt{(p, p-1, p-2, \ldots, 1)}$,

where $b = 4$.

Rotated Trunk

Same as Trunk, but the data are randomly rotated, that is, we sample $\boldsymbol{Q}$ uniformly from the set of p-dimensional rotation matrices, and then set:

- $\boldsymbol{\mu}_0 \leftarrow \boldsymbol{Q}\boldsymbol{\mu}_0$,
- $\boldsymbol{\mu}_1 \leftarrow \boldsymbol{Q}\boldsymbol{\mu}_1$,
- $\boldsymbol{\Sigma} \leftarrow \boldsymbol{Q}\boldsymbol{\Sigma}\boldsymbol{Q}^{\mathsf{T}}$.

Toeplitz

- $\boldsymbol{\mu}_0 = b \times (1, -1, 1, -1, \ldots, 1)$,
- $\boldsymbol{\mu}_1 = -\boldsymbol{\mu}_0$,
- $\boldsymbol{\Sigma}$ is a Toeplitz matrix, where the top row is $\rho^{(0,1,2,\ldots,p-1)}$,

where b is a function of the Toeplitz matrix such that the noise stays constant as dimensionality increases, and $\rho = 0.5$.

3 Classes

Same as Trunk, but with a third mean equal to the zero vector, $\mu_2 = \mathbf{0}$.

Fat Tails

For this setting, each class is actually a mixture of two Gaussians with the same mean (the two classes have the same covariances):

- $\boldsymbol{\mu}_0 = \mathbf{0}$,
- $\boldsymbol{\mu}_1 = (0, \ldots, 0, 1, \ldots, 1)$, where the first $s = 10$ elements are zero,
- $\boldsymbol{\Sigma}_0$ is a matrix with one's on the diagonal, and 0.2 on the off diagonal,
- $\boldsymbol{\Sigma}_1 = 15 \times \boldsymbol{\Sigma}_0$,

and then we randomly rotated as in the rotated Trunk example.

QDA

A generalization of the Toeplitz setting, where the two classes have two different covariance matrices, meaning that the optimal discriminant boundary is quadratic.

- $\boldsymbol{\mu}_0 = b \times (1, -1, 1, -1, \ldots, 1)$,
- $\boldsymbol{\mu}_1 = -\boldsymbol{Q} \times (\boldsymbol{\mu}_0 + 0.1)$,
- $\boldsymbol{\Sigma}_0$ is the same Toeplitz matrix as described above, and
- $\boldsymbol{\Sigma}_1 = \boldsymbol{Q}\boldsymbol{\Sigma}_0\boldsymbol{Q}^\mathsf{T}$.

Outliers

In this dataset, we generate $n/2$ samples from an inlier model, and the remaining $n/2$ samples from an outlier model. For the inlier model, we first generate a random $d \times p$ dimensional orthonormal matrix, V, where $d = p/10$. Then, the first half of the inlier points are generated by $f_{x|0}$, the next half by $f_{x|1}$, and the remaining points generated by $f_{x|\emptyset}$. For the outliers, we sampled their class randomly from a fair Bernoulli distribution:

- $f_{x|0} = \mathcal{N}_d(0, \sigma^2) \times V^\mathsf{T}$,
- $f_{x|1} = \mathcal{N}_d(0, \sigma^2) \times V^\mathsf{T} + b$,
- $f_{x|\emptyset} = \mathcal{N}_p(\mathbf{0}, \sigma^2 \boldsymbol{I})$,
- $f_\emptyset = \mathcal{B}(0.5)$.

where we set $\sigma = 0.1$ and $b = 0.5$.

ALGORITHMS	p < n	2-Class LDA MODELS, p > n			GENERALIZED MODELS, p > n					OTHER TASKS, p > n		ALGORITHM PROPERTIES							ALGORITHMS	REF	NOTES
	LDA model	delta & cov aligned	& cov misaligned	delta & cov misaligned rotated	Fat Tails	>2 Class	QDA Model	Outlier Model	Non-linear	Testing	Regress	Fast	Simple	Theory	Open Source	Dense	2-step/ DL	Super-vised			
kNN	X	X	X	X	X	X		X	X		X		X	X	X	X		X	kNN	1	not considered
HCT	X	X	X									X	X	X			X	X	HCT	14	
LDA o Trace-Ratio	X	X	X	X								X	X	X		X	X	X	LDA o Trace-Ratio	4	
F2M / SDR	X			X		X								X	X	X	X	X	F2M / SDR	10	needs n>p
Deep Learning	X				X	X	X	X	X		X				X	X	X	X	Deep Learning	11	best when n>>p
Vowpal Wabbit	X				X	X		X			X	X			X	X	X	X	Vowpal Wabbit	5	best when n>>p
Ridge Regression	X											X	X	X	X	X		X	Ridge Regression	1	regression
Partial Least Squares											X	X						X	Partial Least Squares	1	regression
Naive Bayes	X	X	X			X						X	X	X	X	X		X	Naive Bayes	1,12	
HDDA	X	X	X	X		X									X	X		X	HDDA	6	
ROAD	X	X											X	X	X			X	ROAD	7,8,9	
LASSO	X	X				X					X	X	X	X	X		X	X	LASSO	3	
kSVM	X	X	X	X	X	X	X	X	X					X	X	X		X	kSVM	1	
Random Forest	X													X	X	X		X	Random Forest	1, 15	
LDA	X											X	X	X	X			X	LDA	1	
LDA o PCA	X	X				X					X	X	X	X	X	X	X	1/2	LDA o PCA	2	
LOL	X	X	X	X	X	X	X	X	X	X	X	X	X	X	X	X	X	X	LOL	*	
FIGURE		2A	2B, 3A	2C, 3B	3C	3D	3E	3F	3G	5A, 5D	5C, 5D	6									

Figure 7: Table of algorithms and their properties for high-dimensional data. Gray elements indicate that results are demonstrated in the Figure labeled in the bottom row. 'X' denotes relatively good performance for a given setting, or has the particular property.

B Theoretical Background

II.A The Classification Problem

Let $(\boldsymbol{X}, Y)$ be a pair of random variables, jointly sampled from $F := F_{\boldsymbol{X},Y} = F_{\boldsymbol{X}|Y}F_Y$. Let $\boldsymbol{X}$ be a multivariate vector-valued random variable, such that its realizations live in p dimensional Euclidean space, $\boldsymbol{x} \in \mathbb{R}^p$. Let Y be a categorical random variable, whose realizations are discrete, $y \in \{0, 1, \dots C\}$. The goal of a classification problem is to find a function $g(\boldsymbol{x})$ such that its output tends to be the true class label y:

$$g^*(\boldsymbol{x}) := \operatorname*{argmax}_{g \in \mathcal{G}} \mathbb{P}[g(\boldsymbol{x}) = y].$$

When the joint distribution of the data is known, then the Bayes optimal solution is:

$$g^*(\boldsymbol{x}) := \operatorname*{argmax}_y f_{y|\boldsymbol{x}} = \operatorname*{argmax}_y f_{\boldsymbol{x}|y} f_y = \operatorname*{argmax}_y \{\log f_{\boldsymbol{x}|y} + \log f_y\} \tag{1}$$

Denote expected misclassification rate of classifier g for a given joint distribution F,

$$L_g^F := \mathbb{E}[g(\boldsymbol{x}) \neq y] := \int \mathbb{P}[g(\boldsymbol{x}) \neq y] f_{\boldsymbol{x},y} d\boldsymbol{x} dy,$$

where $\mathbb{E}$ is the expectation, which in this case, is with respect to F_{XY}. For brevity, we often simply write L_g, and we define $L_* := L_{g^*}$.

II.B Linear Discriminant Analysis (LDA)

Linear Discriminant Analysis (LDA) is an approach to classification that uses a linear function of the first two moments of the distribution of the data. More specifically, let $\mu_j = \mathbb{E}[F_{X|Y=j}]$ denote the class conditional mean, and let $\boldsymbol{\Sigma} = \mathbb{E}[F_X^2]$ denote the joint covariance matrix, and $\pi_j = \mathbb{P}[Y = j]$. Using this notation, we can define the LDA classifier:

$$g_{\text{Lda}}(\boldsymbol{x}) := \operatorname*{argmin}_y \frac{1}{2}(\boldsymbol{x} - \boldsymbol{\mu}_0)^\mathsf{T} \boldsymbol{\Sigma}^{-1} (\boldsymbol{x} - \boldsymbol{\mu}_0) + \mathbb{I}\{Y = y\} \log \pi_y,$$

where $\mathbb{I}\{\cdot\}$ is one when its argument is true, and zero otherwise. Let L_{Lda}^F be the misclassification rate of the above classifier for distribution F. Assuming equal class prior and centered means, $\pi_0 = \pi_1$ and $(\boldsymbol{\mu}_0 + \boldsymbol{\mu}1)/2 = \mathbf{0}$, re-arranging a bit, we obtain

$$g_{\text{Lda}}(\boldsymbol{x}) := \operatorname*{argmin}_y \boldsymbol{x}^\mathsf{T} \boldsymbol{\Sigma}^{-1} \boldsymbol{\mu}_y.$$

In words, the LDA classifier chooses the class for whom the projection of an input vector $\boldsymbol{x}$, onto $\boldsymbol{\Sigma}^{-1}\boldsymbol{\mu}_y$, is maximized. When there are only two classes, this further simplies to

$$g_{2-\text{Lda}}(\boldsymbol{x}) := \mathbb{I}\{\boldsymbol{x}^\mathsf{T} \boldsymbol{\Sigma}^{-1} \boldsymbol{\delta} > 0\},$$

where $\boldsymbol{\delta} = \boldsymbol{\mu}_0 - \boldsymbol{\mu}_1$. Note that the equal class prior and centered means assumptions merely changes the threshold constant from 0 to something else.

II.C LDA Model

A statistical model is a family of distributions indexed by a parameter $\boldsymbol{\theta} \in \boldsymbol{\Theta}$, $\mathcal{F}_{\boldsymbol{\theta}} = \{F_{\boldsymbol{\theta}} : \boldsymbol{\theta} \in \boldsymbol{\Theta}\}$. Consider the special case of the above where $F_{\boldsymbol{X}|Y=y}$ is a multivariate Gaussian distribution, $\mathcal{N}(\boldsymbol{\mu}_y, \boldsymbol{\Sigma})$, where each class has its own mean, but all classes have the same covariance. We refer to this model as the LDA model. Let $\boldsymbol{\theta} = (\boldsymbol{\pi}, \boldsymbol{\mu}, \boldsymbol{\Sigma})$, and let $\boldsymbol{\Theta}_{C-\text{Lda}} = (\triangle_C, \mathbb{R}^{p \times C}, \mathbb{R}_{\succ 0}^{p \times p})$, where $\boldsymbol{\mu} = (\boldsymbol{\mu}_1, \dots, \boldsymbol{\mu}_C)$, $\triangle_C$ is the C dimensional simplex, that is $\triangle_C = \{\boldsymbol{x} : x_i \geq 0 \forall i, \sum_i x_i = 1\}$, and $\mathbb{R}_{\succ 0}^{p \times p}$ is the set of positive definite $p \times p$ matrices. Denote $\mathcal{F}_{\text{Lda}} = \{F_{\boldsymbol{\theta}} : \boldsymbol{\theta} \in \boldsymbol{\Theta}_{\text{Lda}}\}$, dropping the superscript C for brevity where appropriate. The following lemma is well known:

Lemma 1. $L^F_{\texttt{Lda}} = L^F_*$ *for any* $F \in \mathcal{F}_{\texttt{Lda}}$.

Proof. Under the LDA model, the Bayes optimal classifier is available by plugging the explicit distributions into Eq. (1). □

C Projection Based Classifiers

Let $\boldsymbol{A} \in \mathbb{R}^{d\times p}$ be an orthonormal matrix, that is, a matrix that projects p dimensional data into a d dimensional subspace, where $\boldsymbol{A}\boldsymbol{A}^\mathsf{T}$ is the $d \times d$ identity matrix, and $\boldsymbol{A}^\mathsf{T}\boldsymbol{A}$ skis symmetric $p \times p$ matrix with rank d. The question that motivated this work is: what is the best projection matrix that we can estimate, to use to "pre-process" the data prior to applying LDA. Projecting the data $\boldsymbol{x}$ onto a low-dimensional subspace, and the classifying via LDA in that subspace is equivalent to redefining the parameters in the low-dimensional subspace, $\boldsymbol{\Sigma}_A = \boldsymbol{A}\boldsymbol{\Sigma}\boldsymbol{A}^\mathsf{T} \in \mathbb{R}^{d\times d}$ and $\boldsymbol{\delta}_A = \boldsymbol{A}\boldsymbol{\delta} \in \mathbb{R}^d$, and then using $g_{\texttt{Lda}}$. When $C = 2$, $\pi_0 = \pi_1$, and $(\mu_0 + \mu_1)/2 = \mathbf{0}$, this amounts to:

$$g^d_A(x) := \mathbb{I}\{(\boldsymbol{A}\boldsymbol{x})^\mathsf{T}\boldsymbol{\Sigma}_A^{-1}\boldsymbol{\delta}_A > 0\}, \text{ where } \boldsymbol{A} \in \mathbb{R}^{d\times p}. \tag{2}$$

Let $L^d_A := \int \mathbb{P}[g_A(\boldsymbol{x}) = y] f_{\boldsymbol{x},y} d\boldsymbol{x} dy$. Our goal therefore is to be able to choose A for a given parameter setting $\boldsymbol{\theta} = (\boldsymbol{\pi}, \boldsymbol{\delta}, \boldsymbol{\Sigma})$, such that L_A is as small as possible (note that L_A will never be smaller than L_*).

Formally, we seek to solve the following optimization problem:

$$\begin{aligned} \underset{\boldsymbol{A}}{\text{minimize}} \quad & \mathbb{E}[\mathbb{I}\{\boldsymbol{x}^\mathsf{T}\boldsymbol{A}^\mathsf{T}\boldsymbol{\Sigma}_A^{-1}\boldsymbol{\delta}_A > 0\} \neq y] \\ \text{subject to} \quad & \boldsymbol{A} \in \mathbb{R}^{p\times d}, \quad \boldsymbol{A}\boldsymbol{A}^\mathsf{T} = \boldsymbol{I}_{d\times d}, \end{aligned} \tag{3}$$

where $\boldsymbol{I}_{u\times v}$ is the $u\times v$ identity matrix identity, that is, $\boldsymbol{I}(i,j) = 1$ for all $i = j \leq \min(u, v)$, and zero otherwise. Let $\mathcal{A}^d = \{\boldsymbol{A} : \boldsymbol{A} \in \mathbb{R}^{d\times p}, \boldsymbol{A}\boldsymbol{A}^\mathsf{T} = \boldsymbol{I}_{d\times d}\}$, and let $\mathcal{A}_* \subset \mathcal{A}$ be the set of $\boldsymbol{A}$ that minimize Eq. (3), and let $\boldsymbol{A}_* \in \mathcal{A}_*$ (where we dropped the superscript d for brevity). Let $L^*_{\boldsymbol{A}} = L_{\boldsymbol{A}_*}$ be the misclassification rate for any $\boldsymbol{A} \in \mathcal{A}_*$, that is, $L^*_{\boldsymbol{A}}$ is the Bayes optimal misclassification rate for the classifier that composes $\boldsymbol{A}$ with LDA.

In our opinion, Eq. (3) is the simplest supervised manifold learning problem there is: a two-class classification problem, where the data are multivariate Gaussians with shared covariances, the manifold is linear, and the classification is done via LDA. Nonetheless, solving Eq. (3) is difficult, because we do not know how to evaluate the integral analytically, and we do not know any algorithms that are guaranteed to find the global optimum in finite time. This has led to previous work using a surrogate function [**?**]. We proceed by studying a few natural choices for $\boldsymbol{A}$.

III.A Bayes Optimal Projection

Lemma 2. $\delta^\mathsf{T}\boldsymbol{\Sigma}^{-1} \in \mathcal{A}_*$

Proof. Let $\boldsymbol{B} = (\boldsymbol{\Sigma}^{-1}\boldsymbol{\delta})^\mathsf{T} = \boldsymbol{\delta}^\mathsf{T}(\boldsymbol{\Sigma}^{-1})^\mathsf{T} = \boldsymbol{\delta}^\mathsf{T}\boldsymbol{\Sigma}^{-1}$, so that $\boldsymbol{B}^\mathsf{T} = \boldsymbol{\Sigma}^{-1}\boldsymbol{\delta}$, and plugging this in to Eq. (2), we obtain

$$\begin{aligned} g_B(x) &= \mathbb{I}\{\boldsymbol{x}\boldsymbol{B}^\mathsf{T}\boldsymbol{\Sigma}_B^{-1}\boldsymbol{\delta}_B > 0\} \\ &= \mathbb{I}\{\boldsymbol{x}^\mathsf{T}\boldsymbol{\Sigma}^{-1}\boldsymbol{\delta} \times (\boldsymbol{\Sigma}_B^{-1}\boldsymbol{\delta}_B) > 0\} && \text{plugging in } \boldsymbol{B} \\ &= \mathbb{I}\{\boldsymbol{x}^\mathsf{T}\boldsymbol{\Sigma}^{-1}\boldsymbol{\delta}k > 0\} && \text{because } \boldsymbol{\Sigma}_B^{-1}\boldsymbol{\delta}_B > 0. \end{aligned}$$

In other words, letting $\boldsymbol{B}$ be the Bayes optimal projection recovers the Bayes classifier, as it should. Or, more formally, for any $F \in \mathcal{F}_{\texttt{Lda}}$, $L_{\boldsymbol{\delta}^\mathsf{T}\boldsymbol{\Sigma}^{-1}} = L_*$ □

III.B Principle Components Analysis (PCA) Projection

Principle Components Analysis (PCA) finds the directions of maximal variance in a dataset. PCA is closely related to eigendecompositions and singular value decompositions (SVD). In particular, the top principle component of a matrix $\boldsymbol{X} \in \mathbb{R}^{p \times n}$, whose columns are centered, is the eigenvector with the largest corresponding eigenvalue of the centered covariance matrix $\boldsymbol{X}\boldsymbol{X}^{\mathsf{T}}$. SVD enables one to estimate this eigenvector without ever forming the outer product matrix, because SVD factorizes a matrix $\boldsymbol{X}$ into $\boldsymbol{U}\boldsymbol{S}\boldsymbol{V}^{\mathsf{T}}$, where $\boldsymbol{U}$ and $\boldsymbol{V}$ are orthonormal $p \times n$ matrices, and $\boldsymbol{S}$ is a diagonal matrix, whose diagonal values are decreasing, $s_1 \geq s_2 \geq \cdots > s_n$. Defining $\boldsymbol{U} = [\boldsymbol{u}_1, \boldsymbol{u}_2, \ldots, \boldsymbol{u}_n]$, where each $\boldsymbol{u}_i \in \mathbb{R}^p$, then $\boldsymbol{u}_i$ is the i^{th} eigenvector, and s_i is the square root of the i^{th} eigenvalue of $\boldsymbol{X}\boldsymbol{X}^{\mathsf{T}}$. Let $\boldsymbol{A}_d^{\text{Pca}} = [\boldsymbol{u}_1, \ldots, \boldsymbol{u}_d]$ be the truncated PCA orthonormal matrix.

The PCA matrix is perhaps the most obvious choice of a orthonormal matrix for several reasons. First, truncated PCA minimizes the squared error loss between the original data matrix and all possible rank d representations:

$$\underset{A \in \mathbb{R}^{d \times p} : \boldsymbol{A}\boldsymbol{A}^{\mathsf{T}} = \boldsymbol{I}_{d \times d}}{\operatorname{argmin}} \left\| \boldsymbol{X} - \boldsymbol{A}^T \boldsymbol{A} \right\|_F^2 .$$

Second, the ubiquity of PCA has led to a large number of highly optimized numerical libraries for computing PCA (for example, LAPACK [25]).

Moreover, let $\boldsymbol{U}_d = [\boldsymbol{u}_1, \ldots, \boldsymbol{u}_d] \in \mathbb{R}^{p \times d}$, and note that $\boldsymbol{U}_d^{\mathsf{T}}\boldsymbol{U}_d = \boldsymbol{I}_{d \times p}$ and $\boldsymbol{U}_d^{\mathsf{T}}\boldsymbol{U}_d = \boldsymbol{I}_{p \times d}$. Similarly, let $\boldsymbol{U}\boldsymbol{S}\boldsymbol{U}^{\mathsf{T}} = \boldsymbol{\Sigma}$, and $\boldsymbol{U}\boldsymbol{S}^{-1}\boldsymbol{U}^{\mathsf{T}} = \boldsymbol{\Sigma}^{-1}$. Let $\boldsymbol{S}_d$ be the matrix whose diagonal entries are the eigenvalues, up to the d^{th} one, that is $\boldsymbol{S}_d(i,j) = s_i$ for $i = j \leq d$ and zero otherwise. Similarly, $\boldsymbol{\Sigma}_d = \boldsymbol{U}\boldsymbol{S}_d\boldsymbol{U}^{\mathsf{T}} = \boldsymbol{U}_d\boldsymbol{S}_d\boldsymbol{U}_d^{\mathsf{T}}$.

Let $g_{\text{Pca}}^d := g_{A_{\text{Pca}}^d}$, and let $L_{\text{Pca}}^d := L_{A_{\text{Pca}}^d}$. And let $g_{\text{Lda}}^d := \mathbb{I}\{x\boldsymbol{\Sigma}_d^{-1}\boldsymbol{\delta} > 0\}$ be the regularized LDA classifier, that is, the LDA classifier, but sets the bottom $p - d$ eigenvalues to zero.

Lemma 3. *$L_{Pca}^d = L_{RR\text{-}Lda}^d$.*

Proof. Plugging $\boldsymbol{U}_d$ into Eq. (2) for $\boldsymbol{A}$, and considering only the left side of the operand, we have

$$\begin{aligned}
(\boldsymbol{A}\boldsymbol{x})^{\mathsf{T}}\boldsymbol{\Sigma}_A^{-1}\boldsymbol{\delta}_A &= \boldsymbol{x}^{\mathsf{T}}\boldsymbol{A}^{\mathsf{T}}\boldsymbol{A}\boldsymbol{\Sigma}^{-1}\boldsymbol{A}^{\mathsf{T}}\boldsymbol{A}\boldsymbol{\delta}, \\
&= \boldsymbol{x}^{\mathsf{T}}\boldsymbol{U}_d\boldsymbol{U}_d^{\mathsf{T}}\boldsymbol{\Sigma}^{-1}\boldsymbol{U}_d\boldsymbol{U}_d^{\mathsf{T}}\boldsymbol{\delta}, \\
&= \boldsymbol{x}^{\mathsf{T}}\boldsymbol{U}_d\boldsymbol{U}_d^{\mathsf{T}}\boldsymbol{U}\boldsymbol{S}^{-1}\boldsymbol{U}\boldsymbol{U}_d\boldsymbol{U}_d^{\mathsf{T}}\boldsymbol{\delta}, \\
&= \boldsymbol{x}^{\mathsf{T}}\boldsymbol{U}_d\boldsymbol{I}_{d \times p}\boldsymbol{S}^{-1}\boldsymbol{I}_{p \times d}\boldsymbol{U}_d^{\mathsf{T}}\boldsymbol{\delta}, \\
&= \boldsymbol{x}^{\mathsf{T}}\boldsymbol{U}_d\boldsymbol{S}_d^{-1}\boldsymbol{U}_d^{\mathsf{T}}\boldsymbol{\delta}, \\
&= \boldsymbol{x}^{\mathsf{T}}\boldsymbol{\Sigma}_d^{-1}\boldsymbol{\delta}.
\end{aligned}$$

□

The implication of this lemma is that if one desires to implement RR-LDA, rather than first learning the eigenvectors and then learning LDA, one can instead directly implement regularized LDA by setting the bottom $p - d$ eigenvalues to zero.

III.C Linear Optimal Low-Rank (LOL) Projection

The basic idea of LOL is to use both $\boldsymbol{\delta}$ and the top d eigenvectors. Most naïvely, we could simply concatenate the two, $\boldsymbol{A}_{\text{Lol}}^d = [\boldsymbol{\delta}, \boldsymbol{A}_{\text{Pca}}^{d-1}]$. Recall that eigenvectors are orthonormal. To maintain orthonormality, we could easily apply Gram-Schmidt, $\boldsymbol{A}_{\text{Lol}}^d = \text{ORTH}([\boldsymbol{\delta}, \boldsymbol{A}_{\text{Pca}}^{d-1}])$. Both in practice and in theory (as will be shown below), this orthogonalization step does not matter much.

to ensure that they are balanced appropriately, we normalize $\boldsymbol{\delta}$

each vector in $\boldsymbol{\delta}$ to have norm unity. Formally, let $\widetilde{\boldsymbol{\delta}}_j = \boldsymbol{\delta}_j / \|\boldsymbol{\delta}_j\|$, where $\boldsymbol{\delta}_j$ is the j^{th} difference of the mean vector (remember, the number of vectors is equal to $C - 1$, where C is the total number of classes),

and let $\boldsymbol{A}^{d}_{\texttt{Lol}} = [\widetilde{\boldsymbol{\delta}}, \boldsymbol{A}^{d-(C-1)}_{\texttt{Pca}}]$. The eigenvectors are all normalized and orthogonal to one another; to impose orthogonality between $\widetilde{\boldsymbol{\delta}}$ and the eigenvectors, we could use any number of numerically optimized algorithms. However, in practice, orthogonalizing does not matter very much, so we do not bother. We formally demonstrate this below.

D Theoretical Properties of LDA based Classifiers

IV.A LDA is rotationally invariant

For certain classification tasks, the ambient coordinates have intrinsic value, for example, when simple interpretability is desired. However, in many other contexts, interpretability is less important [**?**]. When the exploitation task at hand is invariant to rotations, then we have no reason to restrict our search space to be sparse in the ambient coordinates, rather, for example, we can consider sparsity in the eigenvector basis. Fisherfaces is one example of a rotationally invariant classifier, under certain model assumptions. Let $\boldsymbol{W}$ be a rotation matrix, that is $\boldsymbol{W} \in \mathcal{W} = \{\boldsymbol{W} : \boldsymbol{W}^{\mathsf{T}} = \boldsymbol{W}^{-1} \text{ and } \det(\boldsymbol{W}) = 1\}$. Moreover, let $\boldsymbol{W} \circ F$ denote the distribution F after transformation by an operator $\boldsymbol{W}$. For example, if $F = \mathcal{N}(\boldsymbol{\mu}, \boldsymbol{\Sigma})$ then $\boldsymbol{W} \circ F = \mathcal{N}(\boldsymbol{W}\boldsymbol{\mu}, \boldsymbol{W}\boldsymbol{\Sigma}\boldsymbol{W}^{\mathsf{T}})$.

Definition 1. *A rotationally invariant classifier has the following property:*

$$L^{F}_{g} = L^{\boldsymbol{W}\circ F}_{g}, \qquad F \in \mathcal{F}.$$

In words, the Bayes risk of using classifier g on distribution F is unchanged if F is first rotated, for any $F \in \mathcal{F}$.

Now, we can state the main lemma of this subsection: LDA is rotationally invariant.

Lemma 4. $L^{F}_{Lda} = L^{\boldsymbol{W}\circ F}_{Lda}$, *for any $F \in \mathcal{F}$.*

Proof. LDA simply becomes thresholding $\boldsymbol{x}^{\mathsf{T}}\boldsymbol{\Sigma}^{-1}\boldsymbol{\delta}$. Thus, we can demonstrate rotational invariance by demonstrating that $\boldsymbol{x}^{\mathsf{T}}\boldsymbol{\Sigma}^{-1}\boldsymbol{\delta}$ is rotationally invariant.

$$\begin{aligned}
(\boldsymbol{W}\boldsymbol{x})^{\mathsf{T}}(\boldsymbol{W}\boldsymbol{\Sigma}\boldsymbol{W}^{\mathsf{T}})^{-1}\boldsymbol{W}\boldsymbol{\delta} &= \boldsymbol{x}^{\mathsf{T}}\boldsymbol{W}^{\mathsf{T}}(\boldsymbol{W}\boldsymbol{U}\boldsymbol{S}\boldsymbol{U}^{\mathsf{T}}\boldsymbol{W}^{\mathsf{T}})^{-1}\boldsymbol{W}\boldsymbol{\delta} && \text{by substituting } \boldsymbol{U}\boldsymbol{S}\boldsymbol{U}^{\mathsf{T}} \text{ for } \boldsymbol{\Sigma} \\
&= \boldsymbol{x}^{\mathsf{T}}\boldsymbol{W}^{\mathsf{T}}(\widetilde{\boldsymbol{U}}\boldsymbol{S}\widetilde{\boldsymbol{U}}^{\mathsf{T}})^{-1}\boldsymbol{W}\boldsymbol{\delta} && \text{by letting } \widetilde{\boldsymbol{U}} = \boldsymbol{W}\boldsymbol{U} \\
&= \boldsymbol{x}^{\mathsf{T}}\boldsymbol{W}^{\mathsf{T}}(\widetilde{\boldsymbol{U}}\boldsymbol{S}^{-1}\widetilde{\boldsymbol{U}}^{\mathsf{T}})\boldsymbol{W}\boldsymbol{\delta} && \text{by the laws of matrix inverse} \\
&= \boldsymbol{x}^{\mathsf{T}}\boldsymbol{W}^{\mathsf{T}}\boldsymbol{W}\boldsymbol{U}\boldsymbol{S}^{-1}\boldsymbol{U}^{\mathsf{T}}\boldsymbol{W}^{\mathsf{T}}\boldsymbol{W}\boldsymbol{\delta} && \text{by un-substituting } \boldsymbol{W}\boldsymbol{U} = \widetilde{\boldsymbol{U}} \\
&= \boldsymbol{x}^{\mathsf{T}}\boldsymbol{U}\boldsymbol{S}^{-1}\boldsymbol{U}^{\mathsf{T}}\boldsymbol{\delta} && \text{because } \boldsymbol{W}^{\mathsf{T}}\boldsymbol{W} = \boldsymbol{I} \\
&= \boldsymbol{x}^{\mathsf{T}}\boldsymbol{\Sigma}^{-1}\boldsymbol{\delta} && \text{by un-substituting } \boldsymbol{U}\boldsymbol{S}^{-1}\boldsymbol{U}^{\mathsf{T}} = \boldsymbol{\Sigma}
\end{aligned}$$

□

One implication of this lemma is that we can reparameterize without loss of generality. Specifically, defining $\boldsymbol{W} := \boldsymbol{U}^{\mathsf{T}}$ yields a change of variables: $\boldsymbol{\Sigma} \mapsto \boldsymbol{S}$ and $\boldsymbol{\delta} \mapsto \boldsymbol{U}^{\mathsf{T}}\boldsymbol{\delta} := \boldsymbol{\delta}''$, where $\boldsymbol{S}$ is a diagonal covariance matrix. Moreover, let $\boldsymbol{d} = (\sigma_1, \ldots, \sigma_D)^{\mathsf{T}}$ be the vector of eignevalues, then $\boldsymbol{S}^{-1}\boldsymbol{\delta}' = \boldsymbol{d}^{-1} \odot \widetilde{\boldsymbol{\delta}}$, where $\odot$ is the Hadamard (entrywise) product. The LDA classifier may therefore be encoded by a unit vector, $\widetilde{\boldsymbol{d}} := \frac{1}{m}\boldsymbol{d}^{-1} \odot \widetilde{\boldsymbol{\delta}}'$, and its magnitude, $m := \left\|\boldsymbol{d}^{-1} \odot \widetilde{\boldsymbol{\delta}}\right\|$. This will be useful later.

IV.B Rotation of Projection Based Linear Classifiers g_A

By a similar argument as above, one can easily show that:

$$
\begin{aligned}
(\boldsymbol{AWx})^{\mathsf{T}}(\boldsymbol{AW\Sigma W}^{\mathsf{T}}\boldsymbol{A}^{\mathsf{T}})^{-1}\boldsymbol{AW\delta} &= \boldsymbol{x}^{\mathsf{T}}(\boldsymbol{W}^{\mathsf{T}}\boldsymbol{A}^{\mathsf{T}})(\boldsymbol{AW})\boldsymbol{\Sigma}^{-1}(\boldsymbol{W}^{\mathsf{T}}\boldsymbol{A}^{\mathsf{T}})(\boldsymbol{AW})\boldsymbol{\delta} \\
&= \boldsymbol{x}^{\mathsf{T}}\boldsymbol{Y}^{\mathsf{T}}\boldsymbol{Y}\boldsymbol{\Sigma}^{-1}\boldsymbol{Y}^{\mathsf{T}}\boldsymbol{Y}\boldsymbol{\delta} \\
&= \boldsymbol{x}^{\mathsf{T}}\boldsymbol{Z}\boldsymbol{\Sigma}^{-1}\boldsymbol{Z}^{\mathsf{T}}\boldsymbol{\delta} \\
&= \boldsymbol{x}^{\mathsf{T}}(\boldsymbol{Z\Sigma Z}^{\mathsf{T}})^{-1}\boldsymbol{\delta} = \boldsymbol{x}^{\mathsf{T}}\widetilde{\boldsymbol{\Sigma}}_d^{-1}\boldsymbol{\delta},
\end{aligned}
$$

where $\boldsymbol{Y} = \boldsymbol{AW} \in \mathbb{R}^{d\times p}$ so that $\boldsymbol{Z} = \boldsymbol{Y}^{\mathsf{T}}\boldsymbol{Y}$ is a symmetric $p \times p$ matrix of rank d. In other words, rotating and then projecting is equivalent to a change of basis. The implications of the above is:

Lemma 5. *g_A is rotationally invariant if and only if span($\boldsymbol{A}$)=span($\boldsymbol{\Sigma}_d$). In other words,* PCA *is the only rotationally invariant projection.*

IV.C Chernoff information

We now introduce the notion of the Chernoff information, which serves as our surrogate measure for the Bayes error of any classification procedure given the *projected* data – in the context of this paper the projection is via LOL or PCA. Our discussion of the Chernoff information is under the context of decision rules for hypothesis testing, nevertheless, as evidenced by the fact that the Maximum A Posterior decision rule – equivalently the Bayes classifier – achieves the Chernoff information rate, this distinction between hypothesis testing and classification is mainly for ease of exposition.

Let F_0 and F_1 be two absolutely continuous multivariate distribution in $\Omega \subset \mathbb{R}^d$ with density function f_0 and f_1, respectively. Suppose that $Y_1, Y_2, \ldots, Y_m$ are independent and identically distributed random variables, with Y_i distributed either F_0 or F_1. We are interested in testing the simple null hypothesis $\mathbb{H}_0 \colon F = F_0$ against the simple alternative hypothesis $\mathbb{H}_1 \colon F = F_1$. A test T is a sequence of mapping $T_m \colon \Omega^m \mapsto \{0, 1\}$ such that given $Y_1 = y_1, Y_2 = y_2, \ldots, Y_m = y_m$, the test rejects $\mathbb{H}_0$ in favor of $\mathbb{H}_1$ if $T_m(y_1, y_2, \ldots, y_m) = 1$; similarly, the test rejects $\mathbb{H}_1$ in favor of $\mathbb{H}_0$ if $T_m(y_1, y_2, \ldots, y_m) = 0$. The Neyman-Pearson lemma states that, given $Y_1 = y_1, Y_2 = y_2, \ldots, Y_m = y_m$ and a threshold $\eta_m \in \mathbb{R}$, the likelihood ratio test which rejects $\mathbb{H}_0$ in favor of $\mathbb{H}_1$ whenever

$$
\Big(\sum_{i=1}^{m} \log f_0(y_i) - \sum_{i=1}^{m} \log f_1(y_i)\Big) \leq \eta_m
$$

is the most powerful test at significance level $\alpha_m = \alpha(\eta_m)$, i.e., the likelihood ratio test minimizes the type-II error β_m subject to the contrainst that the type-I error is at most α_m.

Assuming that $\pi \in (0, 1)$ is a prior probability that $\mathbb{H}_0$ is true. Then, for a given $\alpha_m^* \in (0, 1)$, let $\beta_m^* = \beta_m^*(\alpha_m^*)$ be the type-II error associated with the likelihood ratio test when the type-I error is at most α_m^*. The quantity $\inf_{\alpha_m^* \in (0,1)} \pi\alpha_m^* + (1-\pi)\beta_m^*$ is then the Bayes risk in deciding between $\mathbb{H}_0$ and $\mathbb{H}_1$ given the m independent random variables $Y_1, Y_2, \ldots, Y_m$. A classical result of Chernoff [26] states that the Bayes risk is intrinsically linked to a quantity known as the *Chernoff information*. More specifically, let $C(F_0, F_1)$ be the quantity

$$
\begin{aligned}
C(F_0, F_1) &= -\log\Big[\inf_{t\in(0,1)} \int_{\mathbb{R}^d} f_0^t(\boldsymbol{x}) f_1^{1-t}(\boldsymbol{x}) \mathrm{d}\boldsymbol{x}\Big] \\
&= \sup_{t\in(0,1)} \Big[-\log \int_{\mathbb{R}^d} f_0^t(\boldsymbol{x}) f_1^{1-t}(\boldsymbol{x}) \mathrm{d}\boldsymbol{x}\Big]
\end{aligned}
\tag{4}
$$

Then we have

$$
\lim_{m\to\infty} \frac{1}{m} \inf_{\alpha_m^* \in (0,1)} \log(\pi\alpha_m^* + (1-\pi)\beta_m^*) = -C(F_0, F_1). \tag{5}
$$

Thus $C(F_0, F_1)$ is the *exponential* rate at which the Bayes error $\inf_{\alpha_m^* \in (0,1)} \pi\alpha_m^* + (1-\pi)\beta_m^*$ decreases as $m \to \infty$; we also note that the $C(F_0, F_1)$ is independent of π. We also define, for a given $t \in (0, 1)$ the Chernoff divergence $C_t(F_0, F_1)$ between F_0 and F_1 by

$$
C_t(F_0, F_1) = -\log \int_{\mathbb{R}^d} f_0^t(\boldsymbol{x}) f_1^{1-t}(\boldsymbol{x}) \mathrm{d}\boldsymbol{x}.
$$

The Chernoff divergence is an example of a f-divergence as defined in [27]. When $t = 1/2$, $C_t(F_0, F_1)$ is the Bhattacharyya distance between F_0 and F_1.

The result of Eq. (5) can be extended to $K + 1 \geq 2$ hypothesis, with the exponential rate being the minimum of the Chernoff information between any pair of hypothesis. More specifically, let $F_0, F_1, \ldots, F_K$ be distributions on $\mathbb{R}^d$ and let $Y_1, Y_2, \ldots, Y_m$ be independent and identically distributed random variables with distribution $F \in \{F_0, F_1, \ldots, F_K\}$. Our inference task is in determining the distribution of the Y_i among the $K+1$ hypothesis $\mathbb{H}_0 \colon F = F_0, \ldots, \mathbb{H}_K \colon F = F_K$. Suppose also that hypothesis $\mathbb{H}_k$ has *a priori* probability π_k. For any decision rule δ, the risk of δ is $r(\delta) = \sum_k \pi_k \sum_{l \neq k} \alpha_{lk}(\delta)$ where $\alpha_{lk}(\delta)$ is the probability of accepting hypothesis $\mathbb{H}_l$ when hypothesis $\mathbb{H}_k$ is true. Then we have [28]

$$\inf_{\delta} \lim_{m \to \infty} \frac{r(\delta)}{m} = -\min_{k \neq l} C(F_k, F_l). \tag{6}$$

where the infimum is over all decision rule δ, i.e., for any δ, $r(\delta)$ decreases to 0 as $m \to \infty$ at a rate no faster than $\exp(-m \min_{k \neq l} C(F_k, F_l))$.

When the distributions F_0 and F_1 are multivariate normal, that is, $F_0 = \mathcal{N}(\mu_0, \Sigma_0)$ and $F_1 = \mathcal{N}(\mu_1, \Sigma_1)$; then, denoting by $\Sigma_t = t\Sigma_0 + (1-t)\Sigma_1$, we have

$$C(F_0, F_1) = \sup_{t \in (0,1)} \Big(\frac{t(1-t)}{2} (\mu_1 - \mu_2)^\top \Sigma_t^{-1} (\mu_1 - \mu_2) + \frac{1}{2} \log \frac{|\Sigma_t|}{|\Sigma_0|^t |\Sigma_1|^{1-t}} \Big).$$

IV.D Projecting data and Chernoff information

We now discuss how the Chernoff information characterizes the effect a linear transformation A of the data has on classification accuracy. We start with the following simple result whose proof follows directly from Eq. (6).

Lemma 6. *Let $F_0 = \mathcal{N}(\mu_0, \Sigma)$ and $F_1 \sim \mathcal{N}(\mu_1, \Sigma)$ be two multivariate normals with equal covariance matrices. For any linear transformation A, let $F_0^{(A)}$ and $F_1^{(A)}$ denotes the distribution of AX when $X \sim F_0$ and $X \sim F_1$, respectively. We then have*

$$\begin{aligned} C(F_0^{(A)}, F_1^{(A)}) &= \frac{1}{8} (\mu_1 - \mu_0)^\top A^\top (A \Sigma A^\top)^{-1} A (\mu_1 - \mu_0) \\ &= \frac{1}{8} (\mu_1 - \mu_0)^\top \Sigma^{-1/2} \Sigma^{1/2} A^\top (A \Sigma A^\top)^{-1} A \Sigma^{1/2} \Sigma^{-1/2} (\mu_1 - \mu_0) \\ &= \frac{1}{8} \| P_{\Sigma^{1/2} A^\top} \Sigma^{-1/2} (\mu_1 - \mu_0) \|_F^2 \end{aligned} \tag{7}$$

where $P_Z = Z(Z^\top Z)^{-1} Z^\top$ denotes the matrix corresponding to the orthogonal projection onto the columns of Z.

Thus for a classification problem where $X|Y = 0$ and $X|Y = 1$ are distributed multivariate normals with mean μ_0 and μ_1 and the same covariance matrix Σ, Lemma 6 then states that for any two linear transformations A and B, the transformed data AX is to be preferred over the transformed data BX if

$$(\mu_1 - \mu_0)^\top A^\top (A \Sigma A^\top)^{-1} A (\mu_1 - \mu_0) > (\mu_1 - \mu_0)^\top B^\top (B \Sigma B^\top)^{-1} B (\mu_1 - \mu_0).$$

As an example, suppose Σ is diagonal with distinct eigenvalues where the diagonal entries of Σ are in non-increasing order. Denote by $\delta = \mu_1 - \mu_0$ and let $A = \delta^\top$ and $B = e_1^\top = (1, 0, 0, \ldots, 0)$ be the linear transformations for LOL and PCA of X into $\mathbb{R}$. We then have

$$C(F_0^{(A)}, F_1^{(A)}) = \frac{(\delta^\top \delta)^2}{\delta^\top \Sigma \delta} = \frac{(\sum_i \delta_i^2)^2}{\sum_i \delta_i^2 \lambda_i}; \quad C(F_0^{(B)}, F_1^{(B)}) = \frac{\delta_1^2}{\lambda_1}$$

where λ_1 is the largest eigenvalue of Σ. Suppose furthermore that $\delta_1 \leq \delta_2 \leq \cdots \leq \delta_p$ and $\lambda_1 > \lambda_2 > \cdots > \lambda_p$. Then $C(F_0^{(A)}, F_1^{(A)})$ can be lower-bounded as

$$C(F_0^{(A)}, F_1^{(A)}) = \frac{(\sum_i \delta_i^2)^2}{\sum_i \delta_i^2 \lambda_i} \geq \frac{(p\delta_1^2)^2}{p\delta_p^2 \lambda_1}$$

and hence $C(F_0^{(A)}, F_1^{(A)}) > C(F_0^{(B)}, F_1^{(B)})$ provided $p\delta_1^2 \geq \delta_p^2$.

When $A = \begin{bmatrix}\delta \mid e_1 \mid e_2 \cdots \mid e_{d-1}\end{bmatrix}^\top \in \mathbb{R}^{d\times p}$ and $B = \begin{bmatrix}e_1 \mid e_2 \mid \cdots \mid e_d\end{bmatrix}^\top \in \mathbb{R}^{d\times p}$ are the linear transformation for LOL and PCA of X into $\mathbb{R}^d$, we have

$$C(F_0^{(A)}, F_1^{(A)}) = \frac{(\sum_{i=d}^p \delta_i^2)^2}{\sum_{i=d}^p \delta_i^2 \lambda_i} + \sum_{i=1}^{d-1} \frac{\delta_i^2}{\lambda_i}; \quad C(F_0^{(B)}, F_1^{(B)}) = \sum_{i=1}^{d} \frac{\delta_i^2}{\lambda_i}.$$

This can be seen as follows. Let $\xi_{d-1} = \begin{bmatrix}e_1 \mid e_2 \mid \cdots \mid e_{d-1}\end{bmatrix} \in \mathbb{R}^{p\times(d-1)}$ and $\zeta_{d-1} = (\lambda_1\delta_1, \lambda_2\delta_2, \ldots, \lambda_{d-1}\delta_{d-1})^\top \in \mathbb{R}^{d-1}$. Then

$$A\Sigma A^\top = \begin{bmatrix}\delta \mid \xi_{d-1}\end{bmatrix}^\top \Sigma \begin{bmatrix}\delta \mid \xi_{d-1}\end{bmatrix} = \begin{bmatrix}\delta^\top\Sigma\delta & \delta^\top\Sigma\xi_{d-1} \\ \xi_{d-1}^\top\Sigma\delta & \xi_{d-1}^\top\Sigma\xi_{d-1}\end{bmatrix} = \begin{bmatrix}\sum_{i=1}^p \delta_i^2\lambda_i & \zeta_{d-1}^\top \\ \zeta_{d-1} & \Sigma_{d-1}\end{bmatrix} \tag{8}$$

where $\Sigma_{d-1} = \operatorname{diag}(\lambda_1, \lambda_2, \ldots, \lambda_{d-1})$ is the submatrix of Σ corresponding to the eigenvalues $\lambda_1, \lambda_2, \ldots, \lambda_{d-1}$. Using a formula for the inverse of a partitioned matrix, we have

$$\begin{aligned}(A\Sigma A^\top)^{-1} &= \begin{bmatrix}\sum_{i=1}^p \delta_i^2\lambda_i & \zeta_{d-1}^\top \\ \zeta_{d-1} & \Sigma_{d-1}\end{bmatrix}^{-1} \\ &= \begin{bmatrix}\left(\sum_{i=1}^p \delta_i^2\lambda_i - \zeta_{d-1}^\top\Sigma_{d-1}^{-1}\zeta_{d-1}\right)^{-1} & -\left(\sum_i \delta_i^2\lambda_i - \zeta_{d-1}^\top\Sigma_{d-1}^{-1}\zeta_{d-1}\right)^{-1}\zeta_{d-1}^\top\Sigma_{d-1}^{-1} \\ -\Sigma_{d-1}^{-1}\zeta_{d-1}\left(\sum_i \delta_i^2\lambda_i - \zeta_{d-1}^\top\Sigma_{d-1}^{-1}\zeta_{d-1}\right)^{-1} & \Sigma_{d-1}^{-1} + \Sigma_{d-1}^{-1}\zeta_{d-1}\left(\sum_i \delta_i^2\lambda_i - \zeta_{d-1}^\top\Sigma_{d-1}^{-1}\zeta_{d-1}\right)^{-1}\zeta_{d-1}^\top\Sigma_{d-1}^{-1}\end{bmatrix}\end{aligned} \tag{9}$$

Now, $\sum_{i=1}^p \delta_i^2\lambda_i - \zeta_{d-1}^\top\Sigma_{d-1}^{-1}\zeta_{d-1} = \sum_{i=1}^p \delta_i^2 - \sum_{i=1}^{d-1} \delta_i^2\lambda_i = \sum_{i=d}^p \delta_i^2\lambda_i$. Therefore,

$$(A\Sigma A^\top)^{-1} = \begin{bmatrix}\left(\sum_{i=d}^p \delta_i^2\lambda_i\right)^{-1} & -\frac{\zeta_{d-1}^\top\Sigma_{d-1}^{-1}}{\sum_{i=d}^p \delta_i^2\lambda_i} \\ -\frac{\Sigma_{d-1}^{-1}\zeta_{d-1}}{\sum_{i=d}^p \delta_i^2\lambda_i} & \Sigma_{d-1}^{-1} + \frac{\Sigma_{d-1}^{-1}\zeta_{d-1}\zeta_{d-1}^\top\Sigma_{d-1}^{-1}}{\sum_{i=d}^p \delta_i^2\lambda_i}\end{bmatrix}. \tag{10}$$

In addition, $A(\mu_1 - \mu_0) = (\delta^\top\delta, \delta_1, \delta_2, \ldots, \delta_{d-1})^\top = (\delta^\top\delta, \zeta_{d-1}^\top\Sigma_{d-1}^{-1})^\top \in \mathbb{R}^d$. Hence

$$\begin{aligned}(\mu_1 - \mu_0)^\top A^\top (A\Sigma A^\top)^{-1} A(\mu_1 - \mu_0) &= \begin{bmatrix}\delta^\top\delta \mid \zeta_{d-1}^\top\Sigma_{d-1}^{-1}\end{bmatrix} \begin{bmatrix}\left(\sum_{i=d}^p \delta_i^2\lambda_i\right)^{-1} & -\frac{\zeta_{d-1}^\top\Sigma_{d-1}^{-1}}{\sum_{i=d}^p \delta_i^2\lambda_i} \\ -\frac{\Sigma_{d-1}^{-1}\zeta_{d-1}}{\sum_{i=d}^p \delta_i^2\lambda_i} & \Sigma_{d-1}^{-1} + \frac{\Sigma_{d-1}^{-1}\zeta_{d-1}\zeta_{d-1}^\top\Sigma_{d-1}^{-1}}{\sum_{i=d}^p \delta_i^2\lambda_i}\end{bmatrix} \begin{bmatrix}\delta^\top\delta \\ \Sigma_{d-1}^{-1}\zeta_{d-1}\end{bmatrix} \\ &= \frac{(\delta^\top\delta)^2}{\sum_{i=d}^p \delta_i^2\lambda_i} - 2\delta^\top\delta\frac{\zeta_{d-1}^\top\Sigma_{d-1}^{-2}\zeta_{d-1}}{\sum_{i=d}^p \delta_i^2\lambda_i} + \left(\zeta_{d-1}^\top\Sigma_{d-1}^{-3}\zeta_{d-1} + \frac{(\zeta_{d-1}^\top\Sigma_{d-1}^{-2}\zeta_{d-1})^2}{\sum_{i=d}^p \delta_i^2\lambda_i}\right) \\ &= \frac{(\delta^\top\delta - \zeta_{d-1}^\top\Sigma_{d-1}^{-2}\zeta_{d-1})^2}{\sum_{i=d}^p \delta_i^2\lambda_i} + \zeta_{d-1}^\top\Sigma_{d-1}^{-3}\zeta_{d-1} \\ &= \frac{\left(\sum_{i=1}^p \delta_i^2 - \sum_{i=1}^{d-1} \delta_i^2\right)^2}{\sum_{i=d}^p \delta_i^2\lambda_i} + \sum_{i=1}^{d-1} \frac{\delta_i^2}{\lambda_i} = \frac{\left(\sum_{i=d}^p \delta_i^2\right)^2}{\sum_{i=d}^p \delta_i^2\lambda_i} + \sum_{i=1}^{d-1} \frac{\delta_i^2}{\lambda_i}.\end{aligned}$$

The derivation of $C(F_0^{(B)}, F_1^{(B)})$ is straightforward and will be omitted. We therefore have

$$C(F_0^{(A)}, F_1^{(A)}) - C(F_0^{(B)}, F_1^{(B)}) = \frac{\left(\sum_{i=d}^p \delta_i^2\right)^2}{\sum_{i=d}^p \delta_i^2\lambda_i} - \frac{\delta_d^2}{\lambda_d}.$$

D. LDA

From our assumption that $\lambda_d \geq \lambda_{d+1} \geq \cdots \geq \lambda_p$, we have $\sum_{i=d}^p \delta_i^2 \lambda_i \leq \lambda_d \sum_{i=d}^p \delta_i^2$ and hence

$$\frac{\left(\sum_{i=d}^p \delta_i^2\right)^2}{\sum_{i=d}^p \delta_i^2 \lambda_i} \geq \frac{\left(\sum_{i=d}^p \delta_i^2\right)^2}{\lambda_d \sum_{i=d}^p \delta_i^2} = \frac{1}{\lambda_d} \sum_{i=d}^p \delta_i^2 \geq \frac{\delta_d^2}{\lambda_d}$$

and hence $C(F_0^{(A)}, F_1^{(A)}) \geq C(F_0^{(B)}, F_1^{(B)})$ always, and the inequality is strict provided that $\sum_{d+1}^p \delta_d^2 > 0$.

Finally we consider the case where Σ is an arbitrary covariance matrix. Let $\lambda_1 \geq \lambda_2 \geq \cdots \geq \lambda_p$ be the eigenvalues of Σ and let $u_1, u_2, \ldots, u_p$ be the corresponding eigenvectors. For $d \leq p$, let $U_{d-1} = \left[u_1 \mid u_2 \mid \cdots \mid u_{d-1}\right] \in \mathbb{R}^{p \times (d-1)}$ be the matrix whose columns are the eigenvectors $u_1, u_2, \ldots, u_{d-1}$ of Σ. Then the LOL projection matrix into $\mathbb{R}^d$ is given by $A = \left[\delta | U_{d-1}\right]^\top$. We first have

$$A\Sigma A^\top = \left[\delta | U_{d-1}\right]^\top \Sigma \left[\delta | U_{d-1}\right] = \begin{bmatrix} \delta^\top \Sigma & \delta^\top \Sigma U_{d-1} \\ U_{d-1}^\top \Sigma \delta & U_{d-1}^\top \Sigma U_{d-1} \end{bmatrix} = \begin{bmatrix} \delta^\top \Sigma & \delta^\top \Sigma U_{d-1} \\ U_{d-1}^\top \Sigma \delta & \Lambda_{d-1} \end{bmatrix}$$

where $\Lambda_{d-1} = \operatorname{diag}(\lambda_1, \lambda_2, \ldots, \lambda_{d-1})$ is the $(d-1) \times (d-1)$ diagonal matrix formed by the eigenvalues $\lambda_1, \lambda_2, \ldots, \lambda_{d-1}$. Therefore, letting $\gamma = \delta^\top \Sigma \delta - \delta^\top \Sigma U_{d-1} \Lambda_{d-1}^{-1} U_{d-1}^\top \Sigma \delta$, we have

$$\begin{aligned}(A\Sigma A^\top)^{-1} &= \begin{bmatrix} \delta^\top \Sigma \delta & \delta^\top \Sigma U_{d-1} \\ U_{d-1}^\top \Sigma \delta & U_{d-1}^\top \Sigma U_{d-1} \end{bmatrix}^{-1} \\ &= \begin{bmatrix} \gamma^{-1} & -\delta^\top \Sigma U_{d-1} \Lambda_{d-1}^{-1} \gamma^{-1} \\ -\Lambda_{d-1}^{-1} U_{d-1}^\top \Sigma \delta \gamma^{-1} & \left(\Lambda_{d-1} - \frac{U_{d-1}^\top \Sigma \delta \delta^\top \Sigma U_{d-1}}{\delta^\top \Sigma \delta}\right)^{-1} \end{bmatrix}.\end{aligned}$$

The Sherman-Morrison-Woodbury formula then implies

$$\begin{aligned}\left(\Lambda_{d-1} - \frac{U_{d-1}^\top \Sigma \delta \delta^\top \Sigma U_{d-1}}{\delta^\top \Sigma \delta}\right)^{-1} &= \Lambda_{d-1}^{-1} + \frac{\Lambda_{d-1}^{-1} U_{d-1}^\top \Sigma \delta \delta^\top \Sigma U_{d-1} \Lambda_{d-1}^{-1} / (\delta^\top \Sigma \delta)}{1 - \delta^\top \Sigma U_{d-1} \Lambda_{d-1}^{-1} U_{d-1}^\top \Sigma \delta / (\delta^\top \Sigma \delta)} \\ &= \Lambda_{d-1}^{-1} + \frac{\Lambda_{d-1}^{-1} U_{d-1}^\top \Sigma \delta \delta^\top \Sigma U_{d-1} \Lambda_{d-1}^{-1}}{\delta^\top \Sigma \delta - \delta^\top \Sigma U_{d-1} \Lambda_{d-1}^{-1} U_{d-1}^\top \Sigma \delta} \\ &= \Lambda_{d-1}^{-1} + \gamma^{-1} \Lambda_{d-1}^{-1} U_{d-1}^\top \Sigma \delta \delta^\top \Sigma U_{d-1} \Lambda_{d-1}^{-1}\end{aligned}$$

We note that $\Sigma U_{d-1} = U_{d-1} \Lambda_{d-1}$ and $U_{d-1}^\top \Sigma = \Lambda_{d-1} U_{d-1}^\top$ and hence

$$\begin{aligned}\gamma = \delta^\top \Sigma \delta - \delta^\top \Sigma U_{d-1} \Lambda_{d-1}^{-1} U_{d-1}^\top \Sigma \delta &= \delta^\top \Sigma \delta - \delta^\top U_{d-1} \Lambda_{d-1} \Lambda_{d-1}^{-1} \Lambda_{d-1} U_{d-1}^\top \delta \\ &= \delta^\top \Sigma \delta - \delta^\top U_{d-1} \Lambda_{d-1} U_{d-1}^\top \delta = \delta^\top (\Sigma - \Sigma_{d-1}) \delta\end{aligned}$$

where $\Sigma_{d-1} = U_{d-1} \Lambda_{d-1} U_{d-1}^\top$ is the best rank $d-1$ approximation to Σ with respect to any unitaritly invariant norm. In addition,

$$\Lambda_{d-1}^{-1} U_{d-1}^\top \Sigma \delta \delta^\top \Sigma U_{d-1} \Lambda_{d-1}^{-1} = \Lambda_{d-1}^{-1} \Lambda_{d-1} U_{d-1}^\top \delta \delta^\top U_{d-1} \Lambda_{d-1} \Lambda_{d-1}^{-1} = U_{d-1}^\top \delta \delta^\top U_{d-1}.$$

We thus have

$$(A\Sigma A^\top)^{-1} = \begin{bmatrix} \gamma^{-1} & -\delta^\top \Sigma U_{d-1} \Lambda_{d-1}^{-1} \gamma^{-1} \\ -\Lambda_{d-1}^{-1} U_{d-1}^\top \Sigma \delta \gamma^{-1} & \left(\Lambda_{d-1} - \frac{U_{d-1}^\top \Sigma \delta \delta^\top \Sigma U_{d-1}}{\delta^\top \Sigma \delta}\right)^{-1} \end{bmatrix} = \begin{bmatrix} \gamma^{-1} & -\gamma^{-1} \delta^\top U_{d-1} \\ -\gamma^{-1} U_{d-1}^\top \delta & \Lambda_{d-1}^{-1} + \gamma^{-1} U_{d-1}^\top \delta \delta^\top U_{d-1} \end{bmatrix}.$$

Therefore,

$$\begin{aligned}\delta^\top A^\top (A\Sigma A^\top)^{-1} A \delta &= \delta^\top \left[\delta \mid U_{d-1}\right] \begin{bmatrix} \gamma^{-1} & -\gamma^{-1} \delta^\top U_{d-1} \\ -\gamma^{-1} U_{d-1}^\top \delta & \Lambda_{d-1}^{-1} + \gamma^{-1} U_{d-1}^\top \delta \delta^\top U_{d-1} \end{bmatrix} \left[\delta | U_{d-1}\right]^\top \delta \\ &= \left[\delta^\top \delta \mid \delta^\top U_{d-1}\right] \begin{bmatrix} \gamma^{-1} & -\gamma^{-1} \delta^\top U_{d-1} \\ -\gamma^{-1} U_{d-1}^\top \delta & \Lambda_{d-1}^{-1} + \gamma^{-1} U_{d-1}^\top \delta \delta^\top U_{d-1} \end{bmatrix} \begin{bmatrix} \delta^\top \delta \\ U_{d-1}^\top \delta \end{bmatrix} \\ &= \gamma^{-1} (\delta^\top \delta)^2 - 2\gamma^{-1} \delta^\top \delta \delta^\top U_{d-1} U_{d-1}^\top \delta + \delta^\top U_{d-1} (\Lambda_{d-1}^{-1} + \gamma^{-1} U_{d-1}^\top \delta \delta^\top U_{d-1}) U_{d-1}^\top \delta \\ &= \gamma^{-1} (\delta^\top \delta - \delta^\top U_{d-1} U_{d-1}^\top \delta)^2 + \delta^\top U_{d-1} \Lambda_{d-1}^{-1} U_{d-1}^\top \delta \\ &= \gamma^{-1} (\delta^\top (I - U_{d-1} U_{d-1}^\top) \delta)^2 + \delta^\top \Sigma_{d-1}^\dagger \delta\end{aligned}$$

where $\Sigma_{d-1}^{\dagger}$ is the Moore-Penrose pseudo-inverse of Σ_{d-1}. The PCA projection matrix into $\mathbb{R}^d$ is given by $B = U_d^\top$ and hence

$$\delta^\top B^\top (B\Sigma B^\top)^{-1} B\delta = \delta^\top U_d \Lambda_d^{-1} U_d^\top \delta = \delta^\top \Sigma_d^{\dagger} \delta. \tag{11}$$

We thus have

$$\begin{aligned} C(F_0^{(A)}, F_1^{(A)}) - C(F_0^{(B)}, F_1^{(B)}) &= \gamma^{-1}(\delta^\top (I - U_{d-1}U_{d-1}^\top)\delta)^2 - \delta^\top(\Sigma_d^{\dagger} - \Sigma_{d-1}^{\dagger})\delta \\ &= \frac{(\delta^\top (I - U_{d-1}U_{d-1}^\top)\delta)^2}{\delta^\top(\Sigma - \Sigma_{d-1})\delta} - \delta^\top(\Sigma_d^{\dagger} - \Sigma_{d-1}^{\dagger})\delta \\ &\geq \frac{(\delta^\top (I - U_{d-1}U_{d-1}^\top)\delta)^2}{\lambda_d \delta^\top (I - U_{d-1}U_{d-1}^\top)\delta} - \frac{1}{\lambda_d}\delta^\top u_d u_d^\top \delta \\ &= \frac{1}{\lambda_d}\delta^\top (I - U_{d-1}U_{d-1})\delta - \frac{1}{\lambda_d}\delta^\top (U_d U_d^\top - U_{d-1}U_{d-1}^\top)\delta \geq 0 \end{aligned}$$

where we recall that u_d is the d-th column of U_d. Thus $C(F_0^{(A)}, F_1^{(A)}) \geq C(F_0^{(B)}, F_1^{(B)})$ always, and the inequality is strict whenever $\delta^\top (I - U_d U_d^\top)\delta > 0$.

Next we consider the case when $A = \left[\delta | U_{d-1}\right]^\top$ and $B = U_d$ where U_d is an arbitrary $p \times d$ matrix with $U_d^\top U_d = I$, i.e., U_d has d orthonornal columns, and U_{d-1} is the first $d-1$ columns of U_d. A similar derivation to the above yields

$$C(F_0^{(A)}, F_1^{(A)}) = \frac{(\delta^\top \Sigma^{-1/2}(I - V_{d-1}V_{d-1}^\top)\Sigma^{1/2}\delta)^2}{\delta^\top \Sigma^{1/2}(I - V_{d-1}V_{d-1}^\top)\Sigma^{1/2}\delta} + \delta^\top \Sigma^{-1/2} V_{d-1}V_{d-1}^\top \Sigma^{-1/2}\delta \tag{12}$$

$$C(F_0^{(B)}, F_1^{(B)}) = \delta^\top \Sigma^{-1/2} V_d V_d^\top \Sigma^{-1/2}\delta \tag{13}$$

where $V_d V_{d-1}^\top = \Sigma^{1/2} U_d (U_d^\top \Sigma U_d)^{-1} U_d^\top \Sigma^{1/2}$ is the orthogonal projection onto the column space of $\Sigma^{1/2}U_d$. Hence $C(F_0^{(A)}, F_1^{(A)}) > C(F_0^{(B)}, F_1^{(B)})$ if and only if

$$\frac{(\delta^\top \Sigma^{-1/2}(I - V_{d-1}V_{d-1}^\top)\Sigma^{1/2}\delta)^2}{\delta^\top \Sigma^{1/2}(I - V_{d-1}V_{d-1}^\top)\Sigma^{1/2}\delta} > \delta^\top \Sigma^{-1/2}(V_d V_d^\top - V_{d-1}V_{d-1}^\top)\Sigma^{-1/2}\delta.$$

Let $C(F_0^{(A)}, F_1^{(A)})$ and $C(F_0^{(B)}, F_1^{(B)})$ be the Chernoff informations when $A = [\delta \mid U_{d-1}]^\top$ and $B = [\delta \mid U_d]^\top$ where U_{d-1} and U_d contain the eignevectors of the population covariance matrices Σ; similarly, let $\hat{C}(F_0^{(A)}, F_1^{(A)})$ and $\hat{C}(F_0^{(B)}, F_1^{(B)})$ be the Chernoff informations when $A = [\delta \mid \hat{U}_{d-1}]$ and $B = [\delta \mid \hat{U}_d]$ where $\hat{U}_{d-1}$ and $\hat{U}_d$ contain the eigenvectors of the *s*ample covariance matrices $\hat{\Sigma}$. Suppose furthermore that $C(F_0^{(A)}, F_1^{(A)}) > C(F_0^{(B)}, F_1^{(B)})$. Then for sufficiently large n, with high probability, $\hat{C}(F_0^{(A)}, F_1^{(A)}) > \hat{C}(F_0^{(B)}, F_1^{(B)})$.

Finally we consider the case when $B = \tilde{U}_d^\top$ where $\tilde{U}_d$ is the $p \times d$ matrix whose columns are the d largest eigenvectors of the *pooled* covariance matrix $\tilde{\Sigma} = \mathbb{E}[(X - \frac{\mu_0+\mu_1}{2})(X - \frac{\mu_0+\mu_1}{2})^\top]$. Assume, without loss of generality, that $\mu_1 = -\mu_0 = \mu$. We then have

$$\tilde{\Sigma} = \mathbb{E}[XX^\top] = \pi\Sigma + \pi\mu_0\mu_0^\top + (1-\pi)\Sigma + (1-\pi)\mu_1\mu_1^\top = \Sigma + \mu\mu^\top = \Sigma + \tfrac{1}{4}\delta\delta^\top.$$

Therefore

$$(B\Sigma B^\top)^{-1} = \left(\tilde{U}_d^\top \Sigma \tilde{U}_d\right)^{-1} = \left(\tilde{U}_d^\top (\tilde{\Sigma} - \tfrac{1}{4}\delta\delta^\top)\tilde{U}_d\right)^{-1} = \left(\tilde{S}_d - \tfrac{1}{4}\tilde{U}_d^\top \delta\delta^\top \tilde{U}_d\right)^{-1} = \tilde{S}_d^{-1} + \frac{\tilde{S}_d^{-1}\tilde{U}_d^\top \delta\delta^\top \tilde{U}_d \tilde{S}_d^{-1}}{4 - \delta^\top \tilde{U}_d \tilde{S}_d^{-1} \tilde{U}_d^\top \delta}$$

where $\tilde{S}_d$ is the diagonal matrix containing the d largest eigenvalues of $\tilde{\Sigma}$. Hence

$$\begin{aligned} C(F_0^{(B)}, F_1^{(B)}) = \delta^\top B^\top (B\Sigma B^\top)^{-1} B\delta &= \delta^\top \tilde{U}_d \Big(\tilde{S}_d^{-1} + \frac{\tilde{S}_d^{-1}\tilde{U}_d^\top \delta \delta^\top \tilde{U}_d \tilde{S}_d^{-1}}{4 - \delta^\top \tilde{U}_d \tilde{S}_d^{-1} \tilde{U}_d^\top \delta} \Big) \tilde{U}_d^\top \delta \\ &= \delta^\top \tilde{U}_d \tilde{S}_d^{-1} \tilde{U}_d^\top \delta + \frac{(\delta^\top \tilde{U}_d \tilde{S}_d^{-1} \tilde{U}_d^\top \delta)^2}{4 - \delta^\top \tilde{U}_d \tilde{S}_d^{-1} \tilde{U}_d^\top \delta} \\ &= \delta^\top \tilde{\Sigma}_d^\dagger \delta + \frac{(\delta^\top \tilde{\Sigma}_d^\dagger \delta)^2}{4 - \delta^\top \tilde{\Sigma}_d^\dagger \delta} = \frac{4\delta^\top \tilde{\Sigma}_d^\dagger \delta}{4 - \delta^\top \tilde{\Sigma}_d^\dagger \delta}. \end{aligned} \tag{14}$$

where $\tilde{\Sigma}_d = \tilde{U}_d \tilde{S}_d \tilde{U}_d^\top$ is the best rank d approximation to $\tilde{\Sigma} = \Sigma + \frac{1}{4}\delta\delta^\top$.

We recall that the LOL projection $A = [\delta \mid U_{d-1}]^\top$ yields

$$C(F_0^{(A)}, F_1^{(A)}) = \frac{(\delta^\top (I - U_{d-1}U_{d-1}^\top)\delta)^2}{\delta^\top (\Sigma - \Sigma_{d-1})\delta} + \delta^\top \Sigma_{d-1}^\dagger \delta.$$

To illustrate the difference between the LOL projection and that based on the eigenvectors of the *pooled* covariance matrix, consider the following simple example. Let $\Sigma = \mathrm{diag}(\lambda_1, \lambda_2, \ldots, \lambda_p)$ be a diagonal matrix with $\lambda_1 \geq \lambda_2 \geq \cdots \geq \lambda_p$. Also let $\delta = (0, 0, \ldots, 0, s)$. Suppose furthermore that $\lambda_p + s^2/4 < \lambda_d$. Then we have $\tilde{\Sigma}_d = \mathrm{diag}(\lambda_1, \lambda_2, \ldots, \lambda_d, 0, 0, \ldots, 0)$. Thus $\tilde{\Sigma}_d^\dagger = \mathrm{diag}(1/\lambda_1, 1/\lambda_2, \ldots, 1/\lambda_d, 0, 0, \ldots, 0)$ and $\delta^\dagger \tilde{\Sigma}_d^\dagger \delta = 0$. Therefore, $C(F_0^{(B)}, F_1^{(B)}) = 0$.

On the other hand, we have

$$C(F_0^{(A)}, F_1^{(A)}) = \frac{(\delta^\top (I - U_{d-1}U_{d-1}^\top)\delta)^2}{\delta^\top (\Sigma - \Sigma_{d-1})\delta} + \delta^\top \Sigma_{d-1}^\dagger \delta = \frac{s^4}{s^2 \lambda_p} + 0 = s^2/\lambda_p.$$

We can generalize the previous example as follows. Let Σ be a $p \times p$ covariance matrix of the form

$$\Sigma = \begin{bmatrix} \Sigma_d & 0 \\ 0 & \Sigma_d^\perp \end{bmatrix}$$

where Σ_d is a $d \times d$ matrix. Let $\lambda_1 \geq \lambda_2 \geq \cdots \geq \lambda_p$ be the eigenvalues of Σ and suppose furthermore that the eigenvalues of Σ_d are $\lambda_1, \lambda_2, \ldots, \lambda_d$. Let $\gamma = \lambda_d - \lambda_{d+1}$. We now assume that δ are generated randomly as follows. The entries of δ are i.i.d. random variable sampled according to the following distribution. Given an index i, with probability ϵ, $\delta_i = 0$ and with probability $1 - \epsilon$, δ_i is distributed according to a normal distribution with mean $\tau > 0$ and variance σ^2. Then with probability at least ϵ^d, the covariance matrix for $\tilde{\Sigma}$ is of the form

$$\tilde{\Sigma} = \begin{bmatrix} \Sigma_d & 0 \\ 0 & \Sigma_d^\perp + \frac{1}{4}(\tilde{\delta}\tilde{\delta}^\top) \end{bmatrix}$$

where $\tilde{\delta} \in \mathbb{R}^{p-d}$ is formed by excluding the first d elements of δ. Now, if $\lambda_{d+1} + \frac{1}{4}\|\tilde{\delta}\|^2 < \lambda_d$, then the d largest eigenvalues of $\tilde{\Sigma}$ is still $\lambda_1, \lambda_2, \ldots, \lambda_d$, and thus the eigenvectors corresponding to the d largest eigenvalues of $\tilde{\Sigma}$ is the same as that for the d largest eigenvalues of Σ. That is to say,

$$\lambda_{d+1} + \tfrac{1}{4}\|\tilde{\delta}\|^2 < \lambda_d \Longrightarrow \tilde{\Sigma}_d^\dagger = \Sigma_d^\dagger \Longrightarrow \delta^\top \tilde{\Sigma}_d^\dagger \delta = 0 \Longrightarrow C(F_0^{(B)}, F_1^{(B)}) = 0.$$

We now compute the probability that $\lambda_{d+1} + \frac{1}{4}\|\tilde{\delta}\|^2 < \lambda_d$. Suppose for the moment that $\epsilon > 0$ is fixed and do not varies with p. We then have

$$\frac{\sum_{i=d+1}^p \delta_i^2 - (p-d)(1-\epsilon)\tau^2}{\sqrt{(p-d)(2(1-\epsilon)(2\tau^2\sigma^2 + \sigma^4) + \epsilon(1-\epsilon)(\tau^4 + 2\tau^2\sigma^2 + \sigma^4))}} \xrightarrow{\mathrm{d}} N(0,1).$$

Thus, as $p \to \infty$, the probability that $\lambda_{d+1} + \frac{1}{4}\|\tilde{\delta}\|^2 < \lambda_d$ converges to that of

$$\Phi\Big(\frac{4(\lambda_d - \lambda_{d+1}) - (p-d)(1-\epsilon)\tau^2}{\sqrt{(p-d)(2(1-\epsilon)(2\tau^2\sigma^2 + \sigma^4) + \epsilon(1-\epsilon)(\tau^4 + 2\tau^2\sigma^2 + \sigma^4))}} \Big).$$

This probability can be made arbitrarily close to 1 provided that $\lambda_d - \lambda_{d+1} \geq Cp(1-\epsilon)\tau^2$ for all sufficiently large p and for some constant $C > 1/4$. Since the probability that $\delta_1 = \delta_2 = \cdots = \delta_d$ is at least ϵ^d, we thus conclude that for sufficiently large p, with probability at least ϵ^d,

$$C(F_0^{(B)}, F_1^{(B)}) = 0 < C(F_0^{(A)}, F_1^{(A)}).$$

In the case where $\epsilon = \epsilon(p) \to 1$ as $p \to \infty$ such that $p(1-\epsilon) \to \theta$ for some constant K, then the probability that $\lambda_{d+1} + \frac{1}{4}\|\tilde{\delta}\|^2 < \lambda_d$ converges to the probability that

$$\frac{1}{4}\sum_{i=1}^{K} \sigma^2 \chi_1^2(\tau) \geq \lambda_d - \lambda_{d+1}$$

where K is Poisson distributed with mean parameter θ and $\chi_i^2(\tau)$ is the non-central chi-square distribution with one degree of freedom and non-centrality parameter τ. Thus if $\lambda_d - \lambda_{d+1} \geq C\theta\tau^2 \log p$ for sufficiently large p and for some constant C, then this probability can also be made arbitrarily close to 1.

IV.E Finite Sample Performance

We now consider the finite sample performance of LOL and PCA-based classifiers in the high-dimensional setting with small or moderate sample sizes, e.g., when p is comparable to n or when $p \gg n$. Once again we assume that $X|Y = i \sim \mathcal{N}(\mu_i, \Sigma)$ for $i = 0, 1$. Furthermore, we also assume that Σ belongs to the class $\Theta(p, r, k, \tau, \lambda)$ as defined below.

Definition Let $\lambda > 0$, $\tau \geq 1$ and $k \leq p$ be given. Denote by $\Theta(p, r, k, \tau, \lambda, \sigma^2)$ the collection of matrices Σ such that

$$\Sigma = V\Lambda V^\top + \sigma^2 I$$

where V is a $p \times r$ matrix with orthonormal columns and Λ is a $r \times r$ diagonal matrix whose diagonal entries $\lambda_1, \lambda_2, \ldots, \lambda_r$ satisfy $\lambda \geq \lambda_1 \geq \lambda_2 \geq \cdots \geq \lambda_r \geq \lambda/\tau$. In addition, assume also that $|\mathrm{supp}(V)| \leq k$ where $\mathrm{supp}(V)$ denote the non-zero rows of V, i.e., $\mathrm{supp}(V)$ is the subset of $\{1, 2, \ldots, p\}$ such that $V_j \neq 0$ if and only if $j \in \mathrm{supp}(V)$.

We note that in general $r \leq k \ll p$ and $\lambda/\tau \gg \sigma^2$. We then have the following result.

Theorem [29] Suppose there exists constants M_0 and M_1 such that $M_1 \log p \geq \log n \geq M_0 \log \lambda$. Then there exists a constant $c_0 = c_0(M_0, M_1)$ depending on M_0 and M_1 such that for all n and p for which

$$\frac{\tau k}{n} \log \frac{ep}{k} \leq c_0,$$

there exists an estimate $\hat{V}$ of V such that

$$\sup_{\Sigma \in \Theta(p,r,k,\tau,\lambda,\sigma^2)} \mathbb{E}\|\hat{V}\hat{V}^\top - VV^\top\|^2 \leq \frac{Ck(\sigma\lambda + \sigma^2)}{n\lambda^2} \log \frac{ep}{k}$$

where C is a universal constant not depending on p, r, k, τ, λ and σ^2.

We can therefore show that provided that M_0 and M_1 is large enough, and n and p satisfies the condition in the preceding theorem, then provided that the Chernoff information of the population version of LOL is larger than the Chernoff information of the population version of PCA, the expected Chernoff information for the sample version of LOL is also larger than the expected Chernoff information of the sample version of PCA. We emphasize that it is necessary that the LOL and the PCA version both projected into the top $d \leq r$ dimension of the sample covariance matrices.

E The R implementation of LOL

Figure 8 shows the R implementation of `Lol` for binary classification using FlashMatrix [12]. The implementation takes a $D \times I$ matrix, where each column is a training instance and each instance has D features, and outputs a $D \times k$ projection matrix.

```
\Lol~<- function(m, labels, k) {
        counts <- fm.table(labels)
        num.labels <- length(counts$val)
        num.features <- dim(m)[1]
        nv <- k - (num.labels - 1)
        gr.sum <- fm.groupby(m, 1, fm.as.factor(labels, 2), fm.bo.add)
        gr.mean <- fm.mapply.row(gr.sum, counts$Freq, fm.bo.div, FALSE)
        diff <- fm.get.cols(gr.mean, 1) - fm.get.cols(gr.mean, 2)
        svd <- fm.svd(m, nv=0, nu=nv)
        fm.cbind(diff, svd$u)
}
```

Figure 8: The R implementation of LOL.

F Bibliography

[1] R. A. Fisher, "Theory of Statistical Estimation," *Mathematical Proceedings of the Cambridge Philosophical Society*, vol. 22, no. 05, pp. 700–725, Oct. 1925. [Online]. Available: http://journals.cambridge.org/abstract_S0305004100009580 1

[2] Y. LeCun, C. Cortes, and C. Burges, "MNIST handwritten digit database." [Online]. Available: http://yann.lecun.com/exdb/mnist/ 3

[3] P. J. Bickel and E. Levina, "Some theory for Fisher's linear discriminant function, 'naive Bayes', and some alternatives when there are many more variables than observations," *Bernoulli*, vol. 10, no. 6, pp. 989–1010, Dec. 2004. [Online]. Available: http://projecteuclid.org/euclid.bj/1106314847 4, 7

[4] J. Fan, Y. Feng, and X. Tong, "A road to classification in high dimensional space: the regularized optimal affine discriminant," *Journal of the Royal Statistical Society: Series B (Statistical Methodology)*, vol. 74, no. 4, pp. 745–771, Sep. 2012. [Online]. Available: http://doi.wiley.com/10.1111/j.1467-9868.2012.01029.x 5

[5] T. Hastie, R. Tibshirani, and J. H. Friedman, "The Elements of Statistical Learning: Data Mining, Inference, and Prediction," *BeiJing: Publishing House of Electronics Industry*, 2004. 7

[6] P. J. Huber, *Robust Statistics*, ser. Wiley Series in Probability and Statistics. Wiley, 1981, vol. 82, no. 3. [Online]. Available: http://doi.wiley.com/10.1002/9780470434697 7

[7] P. J. Rousseeuw and K. V. Driessen, "A Fast Algorithm for the Minimum Covariance Determinant Estimator," *Technometrics*, vol. 41, no. 3, pp. 212–223, Mar. 1999. [Online]. Available: http://amstat.tandfonline.com/doi/abs/10.1080/00401706.1999.10485670#.VTejtq1Viko

[8] D. Ferrari and Y. Yang, "Maximum L q -likelihood estimation," *The Annals of Statistics*, vol. 38, no. 2, pp. 753–783, apr 2010. [Online]. Available: http://projecteuclid.org/euclid.aos/1266586613 7

[9] E. J. Candès, X. Li, Y. Ma, and J. Wright, "Robust Principal Component Analysis?" *Journal of the ACM*, vol. 58, no. 3, pp. 1–37, Dec. 2009. [Online]. Available: http://dl.acm.org/citation.cfm?id=1970392.1970395http://arxiv.org/abs/0912.3599 7

[10] T. Zhang and G. Lerman, "A Novel M-Estimator for Robust PCA," *Journal of Machine Learning Research*, vol. 15, pp. 749–808, 2014. [Online]. Available: http://jmlr.org/papers/v15/zhang14a.html 7

[11] C. M. Bishop, *Pattern Recognition and Machine Learning*, ser. Information science and statistics. Springer, 2006. [Online]. Available: http://www.library.wisc.edu/selectedtocs/bg0137.pdf 7

[12] D. Zheng, D. Mhembere, J. T. Vogelstein, C. E. Priebe, and R. Burns, "Flashmatrix: Parallel, scalable data analysis with generalized matrix operations using commodity ssds," *arXiv preprint arXiv:1604.06414*, 2016. 7, 27

[13] D. Zheng, D. Mhembere, R. Burns, J. Vogelstein, C. E. Priebe, and A. S. Szalay, "FlashGraph: Processing billion-node graphs on an array of commodity SSDs," in *13th USENIX Conference on File and Storage Technologies (FAST 15)*, Santa Clara, CA, 2015.

[14] D. Zheng, R. Burns, J. Vogelstein, C. E. Priebe, and A. S. Szalay, "An ssd-based eigensolver for spectral analysis on billion-node graphs," *CoRR*, vol. abs/1602.01421, 2016. 7

[15] D. Zheng, D. Mhembere, V. Lyzinski, J. Vogelstein, C. E. Priebe, and R. Burns, "Semi-external memory sparse matrix multiplication on billion-node graphs in a multicore architecture," *CoRR*, vol. abs/1602.02864, 2016. 7

[16] G. M. Amdahl, "Validity of the Single Processor Approach to Achieving Large Scale Computing Capabilities," in *AFIPS Spring Joint Computer Conference, 1967. AFIPS '67 (Spring). Proceedings of the*, vol. 30, 1967, pp. 483–485. [Online]. Available: http://delivery.acm.org/10.1145/1470000/1465560/p483-amdahl.pdf?ip=202.189.127.238{&}id=1465560{&}acc=ACTIVESERVICE{&}key=

CDD1E79C27AC4E65.DE0A32330AE3471B.4D4702B0C3E38B35.4D4702B0C3E38B35{&}CFID=646862329{&}CFTOKEN=33418015{&}{_}{_}acm{_}{_}=1426882996{_}a666a43ab4250317fe0 7

[17] J. Abello, A. L. Buchsbaum, and J. R. Westbrook, "A functional approach to external graph algorithms," in *AlgorithmsESA98*. Springer, 1998, pp. 332–343. 8

[18] E. J. Candès and T. Tao, "Near-Optimal Signal Recovery From Random Projections: Universal Encoding Strategies?" *IEEE Transactions on Information Theory*, vol. 52, no. 12, pp. 5406–5425, dec 2006. [Online]. Available: http://ieeexplore.ieee.org/lpdocs/epic03/wrapper.htm?arnumber=4016283 8

[19] T. Hastie, K. W. Church, P. Li, and K. C. Kdd, "Very sparse random projections," *Proceedings of the 12th ACM SIGKDD international conference on Knowledge discovery and data mining - KDD '06*, p. 287, 2006. [Online]. Available: http://portal.acm.org/citation.cfm?doid=1150402.1150436 8

[20] M. Lopes, L. Jacob, and M. J. Wainwright, "A More Powerful Two-Sample Test in High Dimensions using Random Projection," in *Neural Information Processing Systems*, 2011, pp. 1206–1214. [Online]. Available: http://papers.nips.cc/paper/4260-a-more-powerful-two-sample-test-in-high-dimensions-using-random-projection 9, 12

[21] P. N. Belhumeur, J. P. Hespanha, and D. J. Kriegman, "Eigenfaces vs. fisherfaces: Recognition using class specific linear projection," *IEEE Transactions on Pattern Analysis and Machine Intelligence*, vol. 19, no. 7, pp. 711–720, 1997. 9

[22] S. Mika, G. Ratsch, J. Weston, B. Scholkopf, and K. Mullers, "Fisher discriminant analysis with kernels," in *Neural Networks for Signal Processing IX: Proceedings of the 1999 IEEE Signal Processing Society Workshop (Cat. No.98TH8468)*. IEEE, 1999, pp. 41–48. [Online]. Available: http://ieeexplore.ieee.org/lpdocs/epic03/wrapper.htm?arnumber=788121 9

[23] L. Breiman, "Random forests," *Machine learning*, vol. 45, no. 1, pp. 5–32, 2001. 9

[24] W. K. Allard, G. Chen, and M. Maggioni, "Multi-scale geometric methods for data sets II: Geometric Multi-Resolution Analysis," *Applied and Computational Harmonic Analysis*, vol. 32, no. 3, pp. 435–462, May 2012. [Online]. Available: http://linkinghub.elsevier.com/retrieve/pii/S1063520311000868 9

[25] E. Anderson, Z. Bai, C. Bischof, S. Blackford, J. Demmel, J. Dongarra, J. D. Croz, A. Greenbaum, S. Hammerling, A. McKenney, and D. Sorensen, *LAPACK Users' Guide: Third Edition*. SIAM, 1999. [Online]. Available: https://books.google.com/books?hl=en&lr=&id=AZIvEnr9gCgC&pgis=1 18

[26] H. Chernoff, "A measure of asymptotic efficiency for tests of a hypothesis based on the sum of observations," *Annals of Mathematical Statistics*, vol. 23, pp. 493–507, 1952. 20

[27] I. Csizár, "Information-type measures of difference of probability distributions and indirect observations," *Studia Scientiarum Mathematicarum Hungarica*, vol. 2, pp. 229–318, 1967. 21

[28] C. C. Leang and D. H. Johnson, "On the asymptotics of M-hypothesis bayesian detection," *IEEE Transactions on Information Theory*, vol. 43, pp. 280–282, 1997. 21

[29] T. T. Cai, Z. Ma, and Y. Wu, "Optimal estimation and rank detection for sparse spiked covariance matrices," 2013, arxiv preprint at http://arxiv.org/abs/1305.3235. 26